Application of Relational Models in Mortality Immunization

by

Xinying (Serene) Liang

B.Sc. (Hons.), Simon Fraser University, 2013

Thesis Submitted in Partial Fulfillment

of the Requirements for the Degree of

Master of Science

in the

Department of Statistics and Actuarial Science

Faculty of Science

SIMON FRASER UNIVERSITY

Summer 2015

Approval

Name:	Xinying (Serene) Liang
Degree:	Master of Science (Statistics and Actuarial Science)
Title:	*Application of Relational Models in Mortality Immunization*
Examining Committee:	**Dr. Tim Swartz** (chair) Professor

Dr. Cary Tsai
Senior Supervisor
Associate Professor

Dr. Yi Lu
Supervisor
Associate Professor

Ms. Barbara Sanders
External Examiner
Assistant Professor

Date Defended:	29 July 2015

Abstract

The prediction of future mortality rates by any existing mortality projection models is hardly to be exact, which causes an exposure to mortality and longevity risks for life insurance companies. Since a change in mortality rates has opposite impacts on the surpluses of life insurance and annuity products, hedging strategies of mortality and longevity risks can be implemented by creating an insurance portfolio of both life insurance and annuity products. In this project, we develop a framework of implementing non-size free matching strategies to hedge against mortality and longevity risks. We apply relational models to capture the mortality movements by assuming that the simulated mortality sequence is a proportional and/or a constant change of the expected one, and the amount of the changes varies in the length of the sequence. With the magnitude of the proportional and/or constant changes, we determine the optimal weights of allocating the life insurance and annuity products in a portfolio for mortality immunization according to each of the proposed matching strategies. Comparing the hedging performance of non-size free matching strategies with size free ones proposed by Lin and Tsai (2014), we demonstrate that non-size free matching strategies can hedge against mortality and longevity risks more effectively than the corresponding size free ones.

Keywords: relational model; longevity risk; mortality risk; mortality immunization; hedge effectiveness; surplus

Keywords: Thesis template; Simon Fraser University; time travel paradoxes

Acknowledgements

I would like to express the greatest gratitude to my senior supervisor Dr. Cary Tsai, who encouraged me to pursue a master's degree at Simon Fraser University and supervised me throughout my master's study. I am very lucky to receive professional guidance from a knowledgeable supervisor, who has rich industrial experience, sophisticated knowledge in hedging of mortality and longevity risks, and plenty of patience. Without his enlightening and numerous support, this project is impossible to be completed.

I am very grateful that Dr. Tim Swartz has agreed to be the chair of the examining committee. I want to thank Dr. Yi Lu and Ms. Barbara Sanders for their thorough reviews and valuable comments on this project.

I would like to thank Simon Fraser University; it provides me with opportunities not only to meet with great professors and lovely graduate fellows, especially in Statistics and Actuarial Science department, but also to secure a co-op position in a leading actuarial software developing company.

Last but not least, I would like to express the sincerest gratitude to my family and friends for their endless love, kindest support and ongoing encouragement along the way. I could not go so far and reach current stage without them.

Table of Contents

List of Figures

Chapter 1

Introduction

In this Chapter, we highlight our motivation for doing this project and provide a brief outline of this project. The difference between the actual mortality rates and the predicted mortality rates could lead to financial insolvency and distress for insurance companies. Except for the traditional strategies of transferring mortality and longevity risks through insurance and reinsurance market or capital market, mortality immunization is an important internal strategy for insurance companies to minimize the financial impacts due to the mortality movements.

1.1 Motivations

Although numerous studies on improving the accuracy of mortality rate modelling and forecasting have been done effectively, the uncertainty of future mortality movements cannot be fully captured and reflected in the forecasted mortality rates. Due to the difference between future actual mortality rates and the expected ones (which are used for pricing life insurance and annuity products), the life insurers and annuity providers are exposed to mortality risk (the actual mortality rates are higher than the predicted ones) and longevity risk (the actual mortality rates are lower than the predicted ones), respectively. From historical mortality data in the past decades, a huge improvement has been shown on mortality rates, which could result in financial insolvency for annuity providers, pension programs and social security systems. In addition, unexpected catastrophe, such as earthquakes, tsunamis and hurricanes, would lead to financial distress for life insurers. As a result, it is important to find an effective method of hedging the longevity and mortality risks.

Purchasing mortality-linked securities is one of the most popular strategies for hedging longevity and mortality risks by transferring them to the capital market. Mortality-linked securities which have been studied in academic field include longevity bonds, q-forwards, survivor swaps, annuity futures, mortality options and survivor caps. Although purchasing proper mortality-linked securities can serve for hedging purpose, life insurers and annuity providers have to bear the hedging costs. Natural hedging for mortality risks uses the characteristic of mortality and longevity risks that respond reversely to future mortality movements to hedge against unexpected changes in future benefits. Mortality immunization provides life insurers and annuity providers with natural hedging opportunities by a proper allocation of life insurance and annuity products in a portfolio (Lin and Tsai, 2014). Such natural hedging is an internal strategy with no extra hedging costs involved for an insurer issuing both life insurance and annuity products.

Interest rate immunization which reduces the impact of interest rate changes on the value of an investment portfolio has been widely studied in financial field. Duration and convexity matching strategies are two common approaches to hedging interest rate risks for an interest-sensitive investment portfolio. In the same manner, mortality immunization prevents the negative impact on the value of surplus of an insurance portfolio due to a change in mortality rates. Tsai and Jiang (2011) defined the mortality durations of the prices of insurance and annuity products. Lin and Tsai (2013, 2014) proposed mortality duration and convexity matching strategies by assuming the actual mortality sequence of length k is a uniformly proportional or constant shift of the expected mortality sequence of equal length. With the assumption that the size of the proportional or constant shift is the same over k, the weights of an insurance portfolio of life and annuity products for the duration and convexity matching strategies in Lin and Tsai (2013, 2014) do not depend on the uniform size of the proportional or constant shift because this size will be cancelled out in both numerator and denominator when calculating the weights. We call those strategies size free matching strategies in this project.

In this project, we further develop mortality hedging strategies relaxing the assumption that the size of the proportional or constant shift has to be the same for different lengths of the underlying mortality sequences. In addition, we also extend the matching strategies to a linear relational model for mortality rates with both proportional and constant shifts. Since we assume the mortality movement to be both proportional and constant and the size of the proportional and constant shifts to be varying by different lengths of the underlying mortality sequences, we have to determine the sizes of the proportional and constant shifts for each length. Those strategies are called non-size free matching strategies in this project. We use the Lee-Carter model and USA male mortality data to forecast the deterministic mortality sequence as the expected future mortality rates for pricing, and simulate the stochastic mortality sequences as the actual mortality experience. We also derive closed-form formulas for the non-size free mortality matching strategies, and illustrate the procedure of modeling the surplus of an insurance portfolio based on different matching strategies. We construct two insurance portfolios to compare the hedging performance of non-size free and size free matching strategies, we find that the non-size free matching strategies are more effective than the size free ones.

1.2 Outline

This project consists of 6 chapters. Chapter 2 gives a literature review on previous research on mortality-linked securities and natural hedging for immunizing longevity and mortality risks.

In Chapter 3, we provide some actuarial notations used in this project; then we define some relational models and corresponding durations, convexities and adjustment functions of ${}_kp_x$, which are used to develop the matching strategies in Chapter 4. In addition, we review the Lee-Carter mortality projection model, which is used to forecast the deterministic and stochastic mortality rates for both life insurance and annuity products.

In Chapter 4, we construct a general two-product insurance portfolio of life insurance and annuity products, and develop formulas for calculating the weights for each product according to different assumptions on the adjustment function of ${}_kp_x$. A general procedure of modeling the surplus of the portfolio based on the weights for different strategies is provided. We also specify two insurance portfolios used in Chapter 5 for numerical illustrations.

In Chapter 5, we show the estimates of the parameters in relational models against the length of mortality sequence. Then we compare the hedging performance of non-size free matching strategies to the size free ones from the following aspects: hedge effectiveness for longevity and mortality risks, the 5% VaR (value at risk) and CTE (conditional tail expectation) of the portfolio surplus at time 0, and the 5% VaR of the portfolio surplus against time until portfolio maturity for some specific ages.

Chapter 6 summarizes key results and our findings in this project, and points out the possible topics for future research.

Chapter 2

Literature review

Mortality improvement is a substantial issue over the past decades, which increases the difficulty of forecasting the future mortality rates accurately. Other than interest rate risk, mortality risk is another key problem that life insurers and annuity providers have to face. The discussions on hedging longevity and mortality risks in academic field have been risen in recent years. Current research on mortality has two major directions; one is devoted to developing mortality-linked securities and the other is focused on natural hedging strategies for mortality immunization.

Growing studies have been done in mortality-linked securities including longevity bonds, q-forwards, survivor swaps, annuity futures, mortality options, and survivor caps. Blake and Burrows (2001) argued that governments could contribute to reduce mortality risks directly through improving public health systems. They presented a policy proposal for survivor (or life annuity) bonds and suggested that such survivor (or life annuity) bonds issued by governments can be the vehicle for bond holders to hedge aggregate mortality risks. Lin and Cox (2005) designed and priced mortality bonds and mortality swaps for longevity risk securitization and they also described the strategy of using mortality-based securities to manage longevity risks. Dowd et al. (2006) discussed on the use of survivor swaps to manage mortality risk and on how to price survivor swaps under an incomplete market setting. Menoncin (2008) provided a framework to determine the optimal weight of longevity bond in an investment portfolio that maximizes the investor's wealth at the moment of his/her death. Tsai et al. (2011) proposed an optimal allocation strategy for asset and liability management with longevity bonds under the assumption of both interest rate and mortality rate being stochastic. Coughlan et al. (2011) provided a framework for understanding the longevity risk, calibrating an index-based longevity instrument and evaluating hedge effectiveness. Cairns (2013) developed hedging strategies with an index-based longevity hedging instrument such as a q-forward or deferred longevity swap and evaluated its robustness relative to inclusion of recalibration risk, parameter uncertainty, and Poisson risk. Cairns et al. (2014) decomposed the correlation and hedge effectiveness into key risk factors, and showed that longevity risk can be hedged using index longevity hedges along with other components.

An alternative approach to hedging mortality and longevity risks is mortality immunization: constructing an optimal portfolio with a proper allocation of life insurance and annuity products. However, research regarding morality immunization is limited. Cox and Lin (2007) proposed a natural hedging strategy by combining life insurance and annuities and suggested that implementing such a hedging strategy can help insurance companies manage mortality risk and remain competitive. Based on the study by Cox and Lin (2007), Tsai et al. (2010) introduced a conditional value-at-risk minimization (CVaRM) method to determine an optimal mix of life insurance and annuity products for mortality risk hedging. Wang et al. (2010) and Plat (2011) adopted the concept of mortality duration, and proposed an approximation approach with stochastic mortality rates to obtain the weights of the life insurance and annuity products in an insurance portfolio. Wang et al. (2010) and Plat (2011) used effective mortality duration by assuming a uniformly proportional change in μ (the force of mortality) and q (one-year death probability), respectively. Li and Hardy (2011) and Li and Luo (2012) introduced a key measure called q-duration, and constructed a longevity hedging portfolio of q-forward contracts with such measure. Tsai and Jiang (2011) defined and investigated several mortality durations of the price of a life insurance product under the linear transform of μ. Tsai and Chung (2013) applied linear transform of μ and derived closed-form formulas for size free durations and convexities of the prices of life insurance and annuity products with respect to each of the slope and intercept parameters in the linear transform. Lin and Tsai (2013) defined mortality durations and convexities under the linear transform of μ, q, p (=1-q) respectively, and demonstrated different matching strategies by constructing two-product and three-product insurance portfolios. Lin and Tsai (2014) continued on the study of mortality durations and convexities with respect to a proportional or constant change in μ, q, p, $\ln \mu$, q/p and $\ln(q/p)$, and compared the hedging performance of twenty four duration and convexity matching strategies under a variety of scenarios. Li and Haberman (2015) assessed the effectiveness of mortality immunization by natural hedging strategies under different mortality models.

Chapter 3

Relational models and Lee-Carter model

In this chapter, we introduce three relational models, the linear relational model, proportional relational model and constant relational model which capture the movement of mortality rates, and the well known Lee-Carter model. Relational models provide a framework for deriving the non-size free matching strategies in Chapter 4. With the relational models, we further define the adjustment functions and derive the formulas for estimating the change in ${}_kp_x$ due to mortality movements. We also fit the Lee-Carter model with USA male mortality data from the Human Mortality Database and estimate the model parameters for future mortality prediction. Then we illustrate the deterministic and stochastic mortality paths, which will be used in Chapter 5.

3.1 Notations

The traditional forms of mortality rates are μ (the force of mortality), q (the one-year death probability), $p = 1 - q$ (one-year survival probability) and m (the central death rate). Lee and Carter (1992) and Dowd et al. (2006) modelled the mortality rates in the forms of $\ln(m)$ (the natural logarithm of the central death rate m) and $\ln(q/p) = logit(q)$ (the logic function of q), respectively. Let $U_{x,n} = \{u_x, \cdots, u_{x+n-1}\}$ be a mortality sequence of length n starting age x, where u can be q, $p = 1 - q$, μ, $\ln(\mu)$, m, $\ln(m)$, q/p, or $\ln(q/p)$. We further denote:

- $\mu_{x,n} = \{\mu_x, \cdots, \mu_{x+n-1}\}$: a sequence with each element being the force of mortality;
- $P_{x,n} = \{p_x, \cdots, p_{x+n-1}\}$: a sequence with each element being the one-year survival probability;
- $Q_{x,n} = \{q_x, \cdots, q_{x+n-1}\}$: a sequence with each element being the one-year death probability;
- $\ln(\mu_{x,n}) = \{\ln(\mu_x), \cdots, \ln(\mu_{x+n-1})\}$: a sequence with each element being the natural logarithm of force of mortality;
- $(Q/P)_{x,n} = \{q_x/p_x, \cdots, q_{x+n-1}/p_{x+n-1}\}$: a sequence with each element being the ratio of one-year death probability to one-year survival probability;

- $\ln(Q/P)_{x,n} = \{\ln(q_x/p_x), \cdots, \ln(q_{x+n-1}/p_{x+n-1})\}$: a sequence with each element being the natural logarithm of the ratio of one-year death probability to one-year survival probability.

In this project, we assume $\mu_x(s) = \mu_x(0) \triangleq \mu_x$ for $s \in [0, 1)$. Then $p_x = e^{-\int_0^1 \mu_x(s)ds} = e^{-\mu_x}$ and $m_x = q_x / \int_0^1 {}_s p_x ds = q_x / \int_0^1 e^{-s \cdot \mu_x} ds = \mu_x$, which provide mortality data conversion between μ_x (or m_x) and p_x.

3.2 Relational models

Tsai and Yang (2015) proposed a linear relational model under which there is a linear relationship between two mortality sequences of equal length. Consider the following simple linear model

$$U^*_{x,k} = (1 + \alpha_k) \times U_{x,k} + \beta_k + e_{x,k}.$$

That is, given two sequence of equal length n, $U^*_{x,n}$ and $U_{x,n}$, each subsequence $U^*_{x,k}$ is a proportional shift α_k of the corresponding subsequence $U_{x,k}$ followed by a parallel movement β_k plus an error term $e_{x,k}$ for $k = 1, ..., n$. For example, α_1 and β_1 link the first pair of subsequences (each of length 1), α_2 and β_2 link the first two pairs of subsequences (each of length 2).The estimates $\hat{\alpha}_k$ and $\hat{\beta}_k$ can be obtained by minimizing sum of squares of $e_{x,k}$s (formulas are given in Chapter 4); we place a subscript k on $\hat{\alpha}$ and $\hat{\beta}$ to indicate that both also depend on k (the length of two mortality sequences).

Figure 3.1 illustrates the sequence $U^{2000+n}_{30,40}$ as U^* for the fitting years $2000 + n$ ($n = 1, 5, 10$) against $U^{2000}_{30,40}$ for the base year 2000 and the corresponding linear trends for USA males with different forms of U. The mortality data used for illustrations in this project is from the Human Mortality Database (www.mortality.org). From the figure, we observe an approximately linear relationship between $U^{2000}_{30,40}$ and $U^{2000+n}_{30,40}$ ($n = 1, 5, 10$) for $U = \mu$, P, Q, $\ln(\mu)$, Q/P and $\ln(Q/P)$. In addition, the changes in the slopes of linear trends for different values of n imply a mortality improvement over the years.

Figure 3.1: $U_{30,40}^{2000+n}$ against $U_{30,40}^{2000}$ for the USA male

(a) $U = \mu$

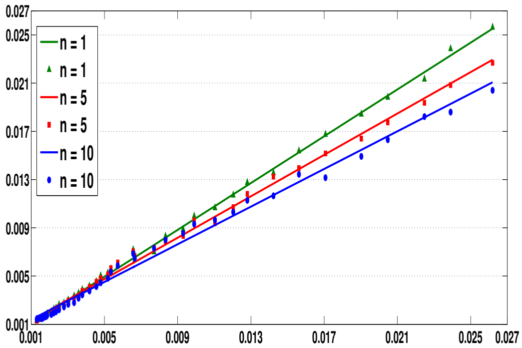

(b) $U = P$

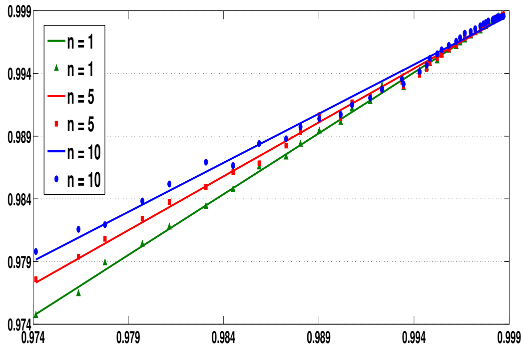

(c) $U = Q$

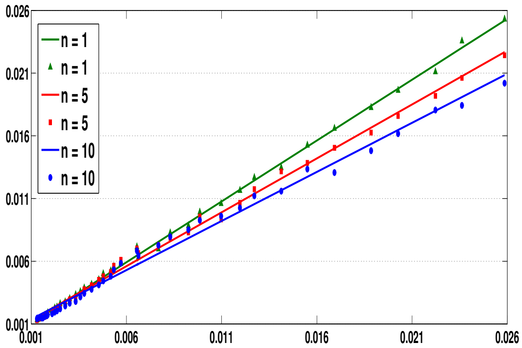

(d) $U = -\ln(\mu)$

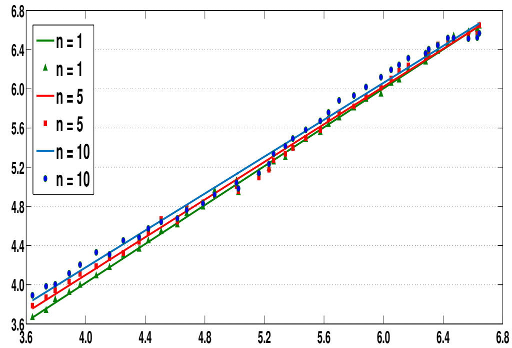

(e) $U = Q/P$

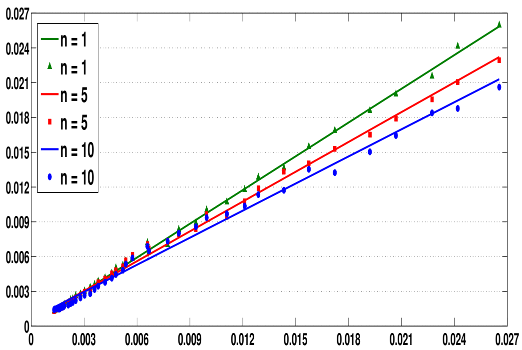

(f) $U = -\ln(Q/P)$

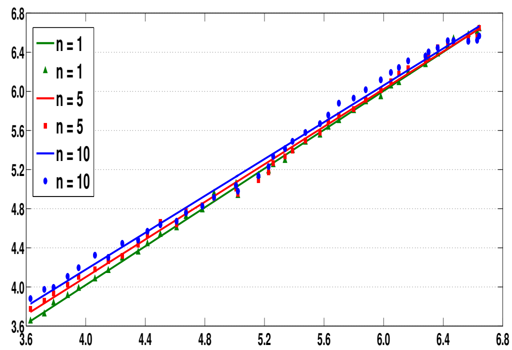

According to the linear relationship we observed between two cohort mortality sequences starting in different year, we presume that a linear relationship between the actual future mortality sequence and expected mortality sequence exists. We assume that the expected mortality rates sequence $U_{x,n}$ is used to price an n-year life or annuity product, which needs ${}_kp_x$, $k = 1, \ldots, n$ for calculating its premium. However, the realized or actual mortality rates sequence, denoted by $U^*_{x,n}$, is different from $U_{x,n}$. We assume the change from $U_{x,k}$ to $U^*_{x,k}$ is linear, proportional or constant for all $k = 1, \ldots, n$, that is, $U^*_{x,k} = (1+\alpha_k) \times U_{x,k} + \beta_k$, $U^*_{x,k} = (1+\alpha_k) \times U_{x,k}$, or $U^*_{x,k} = U_{x,k} + \beta_k$.

When $U_{x,k}$ is shifted proportionally to $U^*_{x,k} = (1+\gamma_k) \cdot U_{x,k}$ or moved by a constant to $U^*_{x,k} = U_{x,k} + \gamma_k$, then the expected ${}_kp_x$ is changed to ${}_kp^*_x = {}_kp_x \cdot f^{\lambda}_{U_{x,k}}(\gamma_k)$ where $f^{\lambda}_{U_{x,k}}(\gamma_k)$ is an adjustment function of ${}_kp_x$ (see Table 1 from Table A.1 in Lin and Tsai (2014)), and $(\lambda, \gamma_k) = (p, \alpha_k)$ or (c, β_k) indicating a proportional or constant change in $U_{x,k}$, respectively.

Table 1. *The adjustment functions* $f^{\lambda}_{U_{x,k}}(\gamma_k)$ *of* ${}_kp_x$ *for* $k \geq 1$ *with* $f^{\lambda}_{U_{x,0}}(\gamma_0) = 1$

U	$f^{p}_{U_{x,k}}(\alpha_k)$	$f^{c}_{U_{x,k}}(\beta_k)$
μ	$\prod_{i=1}^{k}\left[(p_{x+i-1})^{\alpha_k}\right] = ({}_kp_x)^{\alpha_k}$	$\prod_{i=1}^{k}\left[e^{-\beta_k}\right] = e^{-k\times\beta_k}$
Q	$\prod_{i=1}^{k}\left[1-\alpha_k \times \left(\frac{1}{p_{x+i-1}}-1\right)\right]$	$\prod_{i=1}^{k}\left[1-\frac{\beta_k}{p_{x+i-1}}\right]$
P	$\prod_{i=1}^{k}\left[1+\alpha_k\right] = (1+\alpha_k)^{k}$	$\prod_{i=1}^{k}\left[1+\frac{\beta_k}{p_{x+i-1}}\right]$
$\ln(\mu)$	$\prod_{i=1}^{k}\left[(p_{x+i-1})^{[-\ln(p_{x+i-1})]^{\alpha_k}-1}\right]$	$\prod_{i=1}^{k}\left[(p_{x+i-1})^{e^{\beta_k}-1}\right] = ({}_kp_x)^{e^{\beta_k}-1}$
$\frac{Q}{P}$	$\prod_{i=1}^{k}\left[\frac{1}{\alpha_k \times q_{x+i-1}+1}\right]$	$\prod_{i=1}^{k}\left[\frac{1}{\beta_k \times p_{x+i-1}+1}\right]$
$\ln(\frac{Q}{P})$	$\prod_{i=1}^{k}\left[\frac{1}{(q_{x+i-1}/p_{x+i-1})^{\alpha_k} \times q_{x+i-1}+p_{x+i-1}}\right]$	$\prod_{i=1}^{k}\left[\frac{1}{e^{\beta_k} \times q_{x+i-1}+p_{x+i-1}}\right]$

We expand $f^{\lambda}_{U_{x,k}}(\gamma_k)$ with respect to γ_k to

$$f^{\lambda}_{U_{x,k}}(\gamma_k) = f^{\lambda}_{U_{x,k}}(0) + \frac{\partial f^{\lambda}_{U_{x,k}}(\gamma_k)}{\partial \gamma_k}\bigg|_{\gamma_k=0} \times \gamma_k + \frac{\partial^2 f^{\lambda}_{U_{x,k}}(\gamma_k)}{\partial \gamma_k^2}\bigg|_{\gamma_k=0} \times \frac{\gamma_k^2}{2} + R_{f^{\lambda}_{U_{x,k}},3}(\gamma_k) \tag{3.1}$$

with $f^{\lambda}_{U_{x,k}}(0) = 1$ where $R_{f^{\lambda}_{U_{x,k}},3}(\gamma_k) = O(\gamma_k^3)$ is the remainder term with γ_k of order three or higher. Then the change in ${}_kp_x$ due to a proportional or constant movement in $U_{x,k}$ is

$$\triangle\, {}_kp_x(U_{x,k}) \triangleq {}_kp^*_x - {}_kp_x = {}_kp_x\left[\frac{\partial f^{\lambda}_{U_{x,k}}(\gamma_k)}{\partial \gamma_k}\bigg|_{\gamma_k=0} \times \gamma_k + \frac{\partial^2 f^{\lambda}_{U_{x,k}}(\gamma_k)}{\partial \gamma_k^2}\bigg|_{\gamma_k=0} \times \frac{\gamma_k^2}{2} + R_{f^{\lambda}_{U_{x,k}},3}(\gamma_k)\right]. \tag{3.2}$$

Define the duration function as the slope of the tangent line to the $f^{\lambda}_{U_{x,\,k}}(\gamma_k)$ at $\gamma_k = 0$m by

$$d^{\lambda}_{U_{x,\,k}} = \frac{\partial f^{\lambda}_{U_{x,\,k}}(\gamma_k)}{\partial \gamma_k}\Big|_{\gamma_k=0} \tag{3.3}$$

and the convexity function as the curvature of $f^{\lambda}_{U_{x,\,k}}(\gamma_k)$ at $\gamma_k = 0$ by

$$c^{\lambda}_{U_{x,\,k}} = \frac{\partial^2 f^{\lambda}_{U_{x,\,k}}(\gamma_k)}{\partial \gamma_k^2}\Big|_{\gamma_k=0}. \tag{3.4}$$

Then (3.2) can be expressed as

$$\triangle\, {}_kp_x(U_{x,k}) = {}_kp_x\Big[d^{\lambda}_{U_{x,\,k}} \times \gamma_k + c^{\lambda}_{U_{x,\,k}} \times \frac{\gamma_k^2}{2} + R_{f^{\lambda}_{U_{x,\,k}},3}(\gamma_k)\Big]. \tag{3.5}$$

See Tables 2 and 3, from Tables A.2 and A.3 in Lin and Tsai (2014), for the duration and convexity functions of ${}_kp_x$.

Table 2. *The duration functions $d^{\lambda}_{U_{x,\,k}}$ of ${}_kp_x$ for $k \geq 1$ with $d^{\lambda}_{U_{x,\,0}} = 0$*

U	$d^{p}_{U_{x,\,k}}$	$d^{c}_{U_{x,\,k}}$
μ	$\sum_{i=1}^{k}\Big[\ln(p_{x+i-1})\Big] = \ln({}_kp_x),\ {}^{0}\searrow_{-}$	$-\sum_{i=1}^{k}\Big[1\Big] = -k,\ {}^{0}\searrow_{-}$
Q	$-\sum_{i=1}^{k}\Big[\frac{1}{p_{x+i-1}} - 1\Big],\ {}^{0}\searrow_{-}$	$-\sum_{i=1}^{k}\Big[\frac{1}{p_{x+i-1}}\Big],\ {}^{0}\searrow_{-}$
P	$\sum_{i=1}^{k}\Big[1\Big] = k,\ {}_{0}\nearrow^{+}$	$\sum_{i=1}^{k}\Big[\frac{1}{p_{x+i-1}}\Big],\ {}_{0}\nearrow^{+}$
$\ln(\mu)$	$\sum_{i=1}^{k}\Big[\ln(p_{x+i-1}) \times \ln[-\ln(p_{x+i-1})]\Big],\ {}_{0}\nearrow^{+}$	$\sum_{i=1}^{k}\Big[\ln(p_{x+i-1})\Big] = \ln({}_kp_x),\ {}^{0}\searrow_{-}$
$\frac{Q}{P}$	$-\sum_{i=1}^{k}\Big[q_{x+i-1}\Big],\ {}^{0}\searrow_{-}$	$-\sum_{i=1}^{k}\Big[p_{x+i-1}\Big],\ {}^{0}\searrow_{-}$
$\ln(\frac{Q}{P})$	$-\sum_{i=1}^{k}\Big[q_{x+i-1} \times \ln\Big(\frac{q_{x+i-1}}{p_{x+i-1}}\Big)\Big],\ {}_{0}\nearrow^{+}$	$-\sum_{i=1}^{k}\Big[q_{x+i-1}\Big],\ {}^{0}\searrow_{-}$

${}_{0}\nearrow^{+}({}^{0}\searrow_{-})$: increasing (decreasing) in k from 0 at $k = 0$ to positive (negative).

Table 3. *The convexity functions* $c^{\lambda}_{U_{x,\,k}}$ *of* ${}_kp_x$ *for* $k \geq 1$ *with* $c^{\lambda}_{U_{x,\,0}} = 0$

U	$c^{p}_{U_{x,\,k}}$	$c^{c}_{U_{x,\,k}}$
μ	$\Big[d^{p}_{\mu_{x,\,k}}\Big]^2$, ${}_0\nearrow^{+}$	$\Big[d^{c}_{\mu_{x,\,k}}\Big]^2$, ${}_0\nearrow^{+}$
Q	$\Big[d^{p}_{Q_{x,\,k}}\Big]^2 - \sum_{i=1}^{k}\Big(\frac{1}{p_{x+i-1}} - 1\Big)^2$, ${}_0\nearrow^{+}$	$\Big[d^{c}_{Q_{x,\,k}}\Big]^2 - \sum_{i=1}^{k}\Big(\frac{1}{p_{x+i-1}}\Big)^2$, ${}_0\nearrow^{+}$
P	$\Big[d^{p}_{P_{x,\,k}}\Big]^2 - \Big(\sum_{i=1}^{k} 1^2\Big)$, ${}_0\nearrow^{+}$	$\Big[d^{c}_{P_{x,\,k}}\Big]^2 - \sum_{i=1}^{k}\Big(\frac{1}{p_{x+i-1}}\Big)^2$, ${}_0\nearrow^{+}$
$\ln(\mu)$	$\Big[d^{p}_{\ln(\mu_{x,\,k})}\Big]^2 + \Big[\sum_{i=1}^{k} \ln(p_{x+i-1})\,\{\ln\big[-\ln(p_{x+i-1})\big]\}^2\Big]$,	$\Big[d^{c}_{\ln(\mu_{x,\,k})}\Big]^2 + \sum_{i=1}^{k}\Big[\ln(p_{x+i-1})\Big]$,
$\frac{Q}{P}$	$\Big[d^{p}_{\frac{Q_{x,\,k}}{P_{x,\,k}}}\Big]^2 + \sum_{i=1}^{k}\Big(q_{x+i-1}\Big)^2$, ${}_0\nearrow^{+}$	$\Big[d^{c}_{\frac{Q_{x,\,k}}{P_{x,\,k}}}\Big]^2 + \sum_{i=1}^{k}\Big(p_{x+i-1}\Big)^2$, ${}_0\nearrow^{+}$
$\ln(\frac{Q}{P})$	$\Big[d^{p}_{\ln(\frac{Q_{x,\,k}}{P_{x,\,k}})}\Big]^2 - \sum_{i=1}^{k}\Big[q_{x+i-1}\,p_{x+i-1}\Big(\ln\frac{q_{x+i-1}}{p_{x+i-1}}\Big)^2\Big]$	$\Big[d^{c}_{\ln(\frac{Q_{x,\,k}}{P_{x,\,k}})}\Big]^2 - \sum_{i=1}^{k} q_{x+i-1}\,p_{x+i-1}$

${}_0\nearrow^{+}$: increasing in k from 0 at $k = 0$ to positive.

Similarly, when $U_{x,\,k}$ is shifted proportionally to $(1+\alpha_k)\cdot U_{x,\,k}$ and moved by a constant to $U^*_{x,\,k} = (1+\alpha_k)\cdot U_{x,\,k} + \beta_k$, then the expected ${}_kp_x$ is changed to ${}_kp^*_x = {}_kp_x \cdot g_{U_{x,\,k}}(\alpha_k, \beta_k)$ where $g_{U_{x,\,k}}(\alpha_k, \beta_k) = f^{p}_{U_{x,\,k}}(\alpha_k)\cdot f^{c}_{U_{x,\,k}}(\beta_k)$. We expand $g_{U_{x,\,k}}(\alpha_k,\, \beta_k)$ with respect to α_k and β_k to

$$\begin{aligned} g_{U_{x,\,k}}(\alpha_k,\,\beta_k) &= g_{U_{x,\,k}}(0,\,0) + \frac{\partial g_{U_{x,\,k}}(\alpha_k,\,\beta_k)}{\partial \alpha_k}\Big|_{\alpha_k=\beta_k=0} \times \alpha_k + \frac{\partial g_{U_{x,\,k}}(\alpha_k,\,\beta_k)}{\partial \beta_k}\Big|_{\alpha_k=\beta_k=0} \times \beta_k \\ &\quad + \frac{\partial^2 g_{U_{x,\,k}}(\alpha_k,\,\beta_k)}{\partial \alpha_k^2}\Big|_{\alpha_k=\beta_k=0} \times \frac{\alpha_k^2}{2} + \frac{\partial^2 g_{U_{x,\,k}}(\alpha_k,\,\beta_k)}{\partial \beta_k^2}\Big|_{\alpha_k=\beta_k=0} \times \frac{\beta_k^2}{2} \\ &\quad + \frac{\partial^2 g_{U_{x,\,k}}(\alpha_k,\,\beta_k)}{\partial \alpha_k \partial \beta_k}\Big|_{\alpha_k=\beta_k=0} \times \alpha_k\cdot\beta_k + R_{g_{U_{x,\,k}},3}(\alpha_k,\,\beta_k) \end{aligned} \tag{3.6}$$

with $g_{U_{x,\,k}}(0,\,0) = 1$ where $R_{g_{U_{x,\,k}},3}(\alpha_k\,\beta_k)$ is the remainder term with α_k and β_k of order three or higher. By $g_{U_{x,\,k}}(\alpha_k, \beta_k) = f^{p}_{U_{x,\,k}}(\alpha_k)\cdot f^{c}_{U_{x,\,k}}(\beta_k)$, $f^{p}_{U_{x,\,k}}(0) = 1$, $f^{c}_{U_{x,\,k}}(0) = 1$, (3.3) and (3.4), the change in ${}_kp_x$ caused by a proportional shift and a constant movement in $U_{x,\,k}$ is

$$\begin{aligned} \triangle\,{}_kp_x(U_{x,k}) \;\triangleq\; {}_kp^*_x - {}_kp_x &= {}_kp_x\Big[d^{p}_{U_{x,\,k}} \times \alpha_k + d^{c}_{U_{x,\,k}} \times \beta_k \\ &\quad + c^{p}_{U_{x,\,k}} \times \frac{\alpha_k^2}{2} + c^{c}_{U_{x,\,k}} \times \frac{\beta_k^2}{2} + c^{p\,c}_{U_{x,\,k}} \times \alpha_k\beta_k + R_{g_{U_{x,\,k}},3}(\alpha_k, \beta_k)\Big], \end{aligned} \tag{3.7}$$

where $c^{p\,c}_{U_{x\,k}} = d^{p}_{U_{x,\,k}} d^{c}_{U_{x,\,k}}$. Note that (3.7) reduces to (3.5) when α_k or β_k is set to zero.

Consider a general annuity product, the h-year deferred and m-year temporary life annuity-due; its net single premium (NSP) of one unit issued to an insured aged x, using $P_{x,\,h+m-1} =$

$\{p_{x+k-1} : k = 1, 2, \cdots, h+m-1\}$, is denoted as

$$_{h|}\ddot{a}_{x:\,\overline{m}|} = \sum_{k=h}^{h+m-1} {}_{k}p_x \cdot e^{-\delta \cdot k},$$

where $\delta = \ln(1+i)$ is the force of interest and i is the interest rate. There are four common special cases: ${}_nE_x$ (the NSP of the n-year pure endowment) for $(h,\, m) = (n,\, 1)$, $\ddot{a}_{x:\,\overline{n}|}$ (the NSP of the n-year temporary life annuity-due) for $(h,\, m) = (0,\, n)$, ${}_{n|}\ddot{a}_x$ (the NSP of the n-year deferred whole life annuity-due) for $(h,\, m) = (n,\, \infty)$, and $\ddot{a}_x$ (the NSP of the whole life annuity-due) for $(h,\, m) = (0,\, \infty)$.

When $U_{x,\,k}$ is shifted proportionally by an α_k or/and moved constantly by a β_k for $k = 1, \ldots, T$, ${}_{h|}\ddot{a}_{x:\,\overline{m}|}$ becomes ${}_{h|}\ddot{a}^*_{x:\,\overline{m}|} = \sum_{k=h}^{h+m-1} {}_kp^*_x \cdot e^{-\delta \cdot k}$, and the change in ${}_{h|}\ddot{a}_{x:\,\overline{m}|}$ is

$$\triangle\, {}_{h|}\ddot{a}_{x:\,\overline{m}|} \triangleq {}_{h|}\ddot{a}^*_{x:\,\overline{m}|} - {}_{h|}\ddot{a}_{x:\,\overline{m}|} = \sum_{k=h}^{h+m-1} \triangle\, {}_kp_x(U_{x,\,k}) \cdot e^{-\delta \cdot k}, \tag{3.8}$$

where $\triangle\, {}_kp_x(U_{x,\,k})$ is given by (3.5) or (3.7).

3.3 Lee-Carter model

The Lee-Carter model is the most popular method in literature for predicting future mortality rates. In this project, we use the Lee-Carter model to forecast deterministic future mortality rates sequence as the expected mortality one for pricing, and generate stochastic mortality rates sequences as the realized ones for simulation. According to Lee and Carter (1992), the natural logarithm of central death rates can be expressed as

$$ln(m_{x,t}) = a_x + b_x \times k_t + \varepsilon_{x,t}, \qquad x = x_0, ..., x_0 + m - 1, \qquad t = t_0, ..., t_0 + n - 1, \tag{3.9}$$

where

- a_x is the long term average of the natural logarithm of central death rates for age x,
- k_t is the index of the mortality level in specific year t,
- b_x is the reaction of age specific mortality to the year specific factor k_t for age x, and
- $\varepsilon_{x,t}$ is the model error and $\varepsilon_{x,t} \overset{iid}{\sim} \mathrm{N}(0,\, \sigma^2_{\varepsilon_x})$ for all t.

There are two constrains,

- $\sum_x b_x = 1, and$
- $\sum_t k_t = 0.$

According to these two constrains, the sum of the natural logarithm of central death rates over a given year span $[t_0, t_0 + n - 1]$ can be expressed as

$$\sum_{t=t_0}^{t_0+n-1} ln(m_{x,t}) = n \times a_x + b_x \times \sum_{t=t_0}^{t_0+n-1} k_t = n \times a_x, \tag{3.10}$$

and

$$\sum_{x=x_0}^{x_0+m-1} [ln(m_{x,t}) - a_x] = k_t \times \sum_{x=x_0}^{x_0+m-1} b_x. \tag{3.11}$$

Given a dataset $ln(m_{x,t})$ with age span $[x_0,\ x_0 + m - 1]$ and year span $[t_0,\ t_0 + n - 1]$, the estimates of $\widehat{a}_x$, $\widehat{k}_t$, $\widehat{\theta}$ and $\widehat{b}_x$ can be obtained as follows:

- $$\widehat{a}_x = \frac{\sum_{t=t_0}^{t_0+n-1} ln(m_{x,t})}{n}, \tag{3.12}$$

  where $x = x_0, x_0 + 1, ..., x_0 + m - 1$;

- $$\widehat{k}_t = \sum_{x=x_0}^{x_0+m-1} [ln(m_{x,t}) - \widehat{a}_x], \tag{3.13}$$

  where $t = t_0, t_0 + 1, ..., t_0 + n - 1$;

- $\widehat{b}_x$ can be obtained by regressing $\ln(m_{x,t}) - \hat{a}_x$ on $\hat{k}_t$;

- assume that $\hat{k}_t$ follows a random walk with drift θ, that is, $\widehat{k}_t = \widehat{k}_{t-1} + \theta + \epsilon_t$ and $\epsilon_t \overset{iid}{\sim}$ $N(0,\ \sigma_\epsilon^2)$ for all t, and then θ can be estimated as

$$\widehat{\theta} = \frac{1}{n-1} \sum_{t=t_0+1}^{t_0+n-1} (\widehat{k}_t - \widehat{k}_{t-1}) = \frac{\widehat{k}_{t_0+n-1} - \widehat{k}_{t_0}}{n-1}. \tag{3.14}$$

Figure 3.2 shows $\hat{a}_x$, the average age-specific mortality factor from age 20 to 100 ($x_0 = 20$ and $m = 81$) based on the USA males mortality rates from year 1960 to year 2010 ($t_0 = 1960$ and $n = 51$) from Human Mortality Database (www.mortality.org), which data set is used throughout this project. From Figure 3.2 we can find that the average age-specific mortality factor takes negative value for all ages, and it stays stable from age 20 to 30 then keep increasing constantly, which implies that the average of the natural logarithm of central death rates increases in age x.

Figure 3.3 displays $\hat{b}_x$, the age-specific reaction to k_t from age 20 to 100 ($x_0 = 20$ and $m = 81$) based on the same mortality data set from year 1960 to year 2010 ($t_0 = 1960$ and $n = 51$). From Figure 3.3 we can see that $\hat{b}_x$ first decreases from age 20 to 30, and then increases until it reaches a peak at around age 62, and finally keeps decreasing until the eldest age. Furthermore, the $\hat{b}_x$s generally react positively to $\hat{k}_t$ except for the age 97 and above.

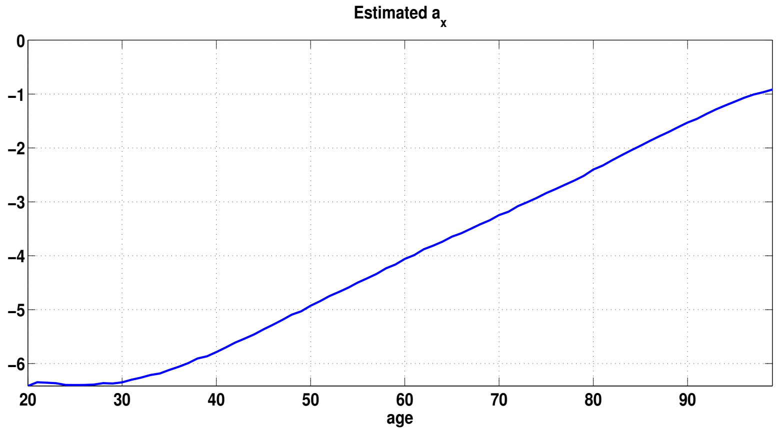

Figure 3.2: $\hat{a}_x$, the average age-specific mortality factor

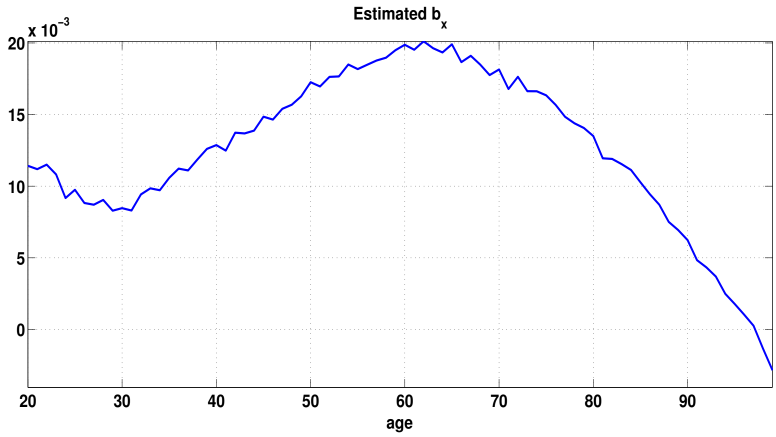

Figure 3.3: $\hat{b}_x$, the age-specific reaction to $\hat{k}_t$

Figure 3.3 illustrates $\hat{k}_t$, the general mortality level in year t based on the same mortality data set from year 1960 to year 2010 ($t_0 = 1960$ and $n = 51$). From Figure 3.3 we can observe a slight increase from 1960 to 1968, followed by a decreasing trend.

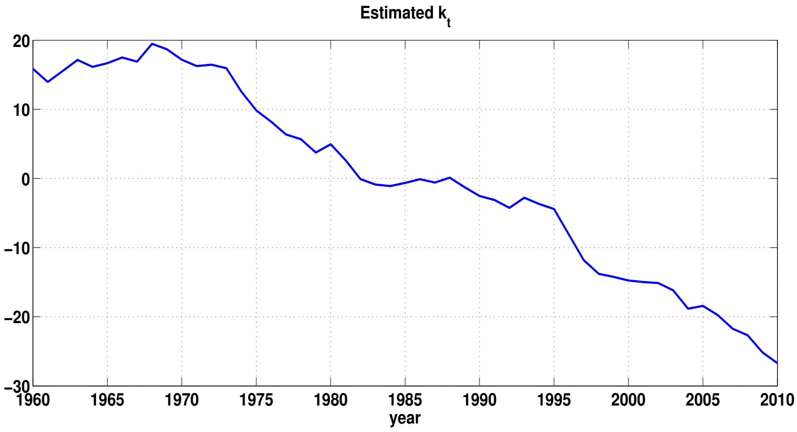

Figure 3.4: $\hat{k}_t$, the general mortality level in year t

Denote $\hat{m}_{x,t_0+n-1+\tau}$ and $\hat{q}_{x,t_0+n-1+\tau}$ the deterministic central death rate and one-year death probability, respectively, for age x in year $t_0 + n - 1 + \tau$; then

$$ln(\hat{m}_{x,t_0+n-1+\tau}) = \hat{a}_x + \hat{b}_x \times (\hat{k}_{t_0+n-1} + \tau \times \hat{\theta}), \tag{3.15}$$

and

$$\hat{q}_{x,t_0+n-1+\tau} = 1 - exp[-exp(\hat{a}_x + \hat{b}_x \times (\hat{k}_{t_0+n-1} + \tau \times \hat{\theta}))], \tag{3.16}$$

$\tau = 1, 2, ...$ Similarly, denote $\tilde{m}_{x,t_0+n-1+\tau}$ and $\tilde{q}_{x,t_0+n-1+\tau}$ the stochastic central death rate and one-year death probability, respectively, for age x in year $t_0 + n - 1 + \tau$; then

$$ln(\tilde{m}_{x,t_0+n-1+\tau}) = \hat{a}_x + \hat{b}_x \times (\hat{k}_{t_0+n-1} + \tau \times \hat{\theta} + \sum_{t=t_0+n}^{t_0+n-1+\tau} \epsilon_t) = ln(\hat{m}_{x,t_0+n-1+\tau}) + \hat{b}_x \times \sum_{t=t_0+n}^{t_0+n-1+\tau} \epsilon_t, \tag{3.17}$$

and

$$\tilde{q}_{x,t_0+n-1+\tau} = 1 - exp[-exp(ln(\hat{m}_{x,t_0+n-1+\tau}) + \hat{b}_x \times \sum_{t=t_0+n}^{t_0+n-1+\tau} \epsilon_t)], \tag{3.18}$$

where the estimate of the variance of error terms ϵ_t is

$$\hat{\sigma}_\epsilon^2 = \frac{1}{n-2} \sum_{t=t_0+1}^{t_0+n-1} \epsilon_t^2 = \frac{\sum_{t=t_0+1}^{t_0+n-1} (\hat{k}_t - \hat{k}_{t-1} - \hat{\theta})^2}{n-2}. \tag{3.19}$$

Moreover, the estimate of the variance of the natural logarithm of the stochastic central death rate, $\hat{\sigma}^2(ln(\tilde{m}_{x,t_0+n-1+\tau}))$, is given by

$$\hat{\sigma}^2(ln(\tilde{m}_{x,t_0+n-1+\tau})) = \tau \times \hat{b}_x^2 \times \hat{\sigma}_\epsilon^2. \tag{3.20}$$

A $100(1-\alpha)\%$ predictive interval on $\hat{q}_{x,t_0+n-1+\tau}$ is

$$1 - exp[-exp(ln(\hat{m}_{x,t_0+n-1+\tau}) \pm z_{\frac{\alpha}{2}} \times \hat{\sigma}^2(ln(\tilde{m}_{x,t_0+n-1+\tau})))]. \tag{3.21}$$

Figure 3.5 shows the projected mortality rates and 95% predictive intervals for the selected cohorts currently aged 20, 40 and 60, based on the USA males mortality data set from year 1960 to year 2010. According to the three graphs in Figure 3.5 , we can see that the deterministic mortality rates have an increasing trend for cohorts. The predictive intervals are narrow at the beginning and then the intervals get wider as age increases, but they begin to shrink when the age is approaching to 80. Paying attention to the mortality rates, we observe that the younger cohort has the lower mortality level when they reach the same age as the elder cohort, which implies a mortality improvement over years.

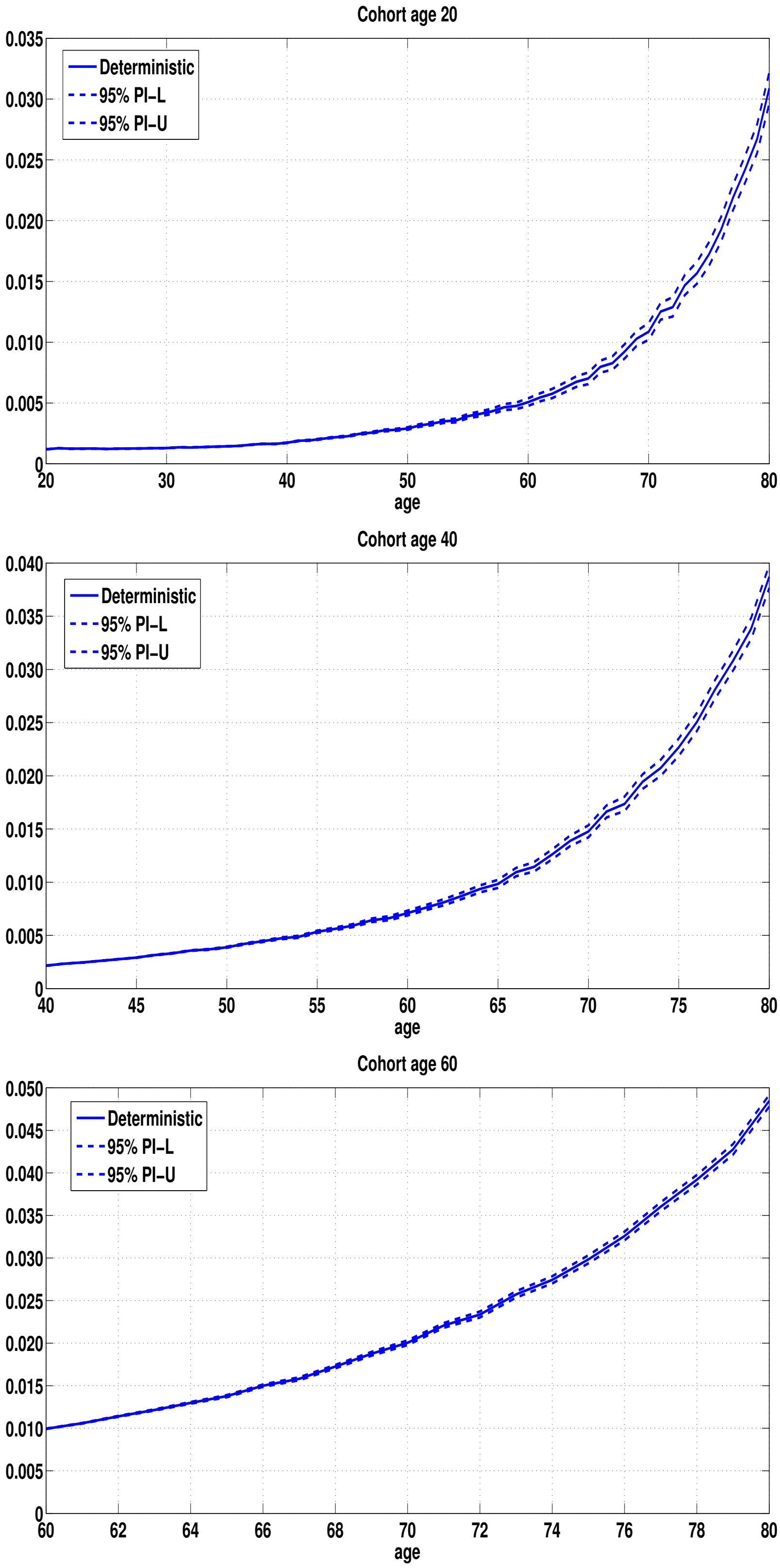

Figure 3.5: Deterministic and 95% predictive intervals on cohort mortality rates

Chapter 4

Matching strategies for mortality immunization

In this chapter, we introduce the matching strategies for mortality immunization for a life insurance portfolio consisting of life insurance and annuity products. We first derive the formulas for determining the proper weights according to different matching strategies and prove that some of the matching strategies result in the same weight if $U = \mu = -\ln P$. Then we focus on two portfolios, PFL^{TP} (the m-payment and n-year term life insurance and the m-payment and n-year pure endowment) and PFL^{WA} (the m-payment whole life insurance and the m-payment and n-year deferred whole life annuity), which are used in Chapter 5 for numerical illustrations. Lastly, we summarize the procedure of modeling surpluses.

4.1 Matching strategies in general

Consider a life insurance portfolio PFL^{LA} consisting of discrete life insurance and an annuity with weights w_L and $w_A = 1 - w_L$, respectively; if the weights w_L and w_A are out of the range of $[0, 1]$, then the portfolio is infeasible. The weighted surplus at time 0 is

$$_0S^{LA}_{x:\,m,\,n} = w_L \cdot {_0S}[P^L_{x:\,m,\,n}] + (1 - w_L) \cdot {_0S}[P^A_{x:\,m,\,n}] = 0,$$

where $1 \le m \le n$, ${_0S}[P^L_{x:\,m,\,n}] = P^L_{x:\,m,\,n} \cdot \ddot{a}_{x:\,\overline{m}|} - A_{x,\,n} = 0$ is the surplus at time 0 for a discrete m-payment and n-year life insurance issued to an insured aged x with the actuarial present value of benefits, $A_{x,\,n}$, and the NLP (net level premium), $P^L_{x:\,m,\,n} = A_{x,\,n}/\ddot{a}_{x:\,\overline{m}|}$, and ${_0S}[P^A_{x:\,m,\,n}] = P^A_{x:\,m,\,n} \cdot \ddot{a}_{x:\,\overline{m}|} - a_{x,\,n} = 0$ is the surplus at time 0 for an m-payment and n-year annuity issued to an annuity recipient aged x with the actuarial present value of benefits, $a_{x,\,n}$, and the NLP, $P^A_{x:\,m,\,n} = a_{x,\,n}/\ddot{a}_{x:\,\overline{m}|}$.

When $U_{x,\,k}$ is shifted proportionally by an α_k or/and moved constantly by a β_k for $k = 1, \ldots, n$, all $\ddot{a}_{x:\,\overline{m}|}$, $A_{x,\,n}$ and $a_{x,\,n}$ change to $\ddot{a}^*_{x:\,\overline{m}|}$, $A^*_{x,\,n}$ and $a^*_{x,\,n}$, respectively, whereas both $P^L_{x:\,m,\,n}$ and $P^A_{x:\,m,\,n}$ are predetermined and unchanged. The resulted surpluses are ${_0S}[P^{L,*}_{x:\,m,\,n}] = P^L_{x:\,m,\,n} \cdot \ddot{a}^*_{x:\,\overline{m}|} - A^*_{x,\,n}$ and ${_0S}[P^{A,*}_{x:\,m,\,n}] = P^A_{x:\,m,\,n} \cdot \ddot{a}^*_{x:\,\overline{m}|} - a^*_{x,\,n}$. Thus, ${_0S}^{LA}$ becomes ${_0S}^{LA,*}_{x:\,m,\,n}$, and the change in ${}_0S^{LA}_{x:\,m,\,n}$ is

$$\triangle\,{}_0S^{LA}_{x:\,m,\,n} \triangleq {}_0S^{LA,\,*}_{x:\,m,\,n} - {}_0S^{LA}_{x:\,m,\,n} = w_L \cdot \triangle\,{}_0S[P^L_{x:\,m,\,n}] + (1-w_L)\cdot \triangle\,{}_0S[P^A_{x:\,m,\,n}],$$

where $\triangle\,{}_0S[P^L_{x:\,m,\,n}] \triangleq {}_0S^*[P^L_{x:\,m,\,n}] - {}_0S[P^L_{x:\,m,\,n}]$ and $\triangle\,{}_0S[P^A_{x:\,m,\,n}] \triangleq {}_0S^*[P^A_{x:\,m,\,n}] - {}_0S[P^A_{x:\,m,\,n}]$. The change in portfolio surplus $\triangle\,{}_0S^{LA}_{x:\,m,\,n}$ is equivalent to the negative of the change in reserve. Our goal is to find the weight $\hat{w}_L$ such that $\triangle\,{}_0S^{LA}_{x:\,m,\,n} = 0$ (that is, the life insurance portfolio is immunized with respect to a change in mortality rates). Then $\hat{w}_L$ can be solved as

$$\hat{w}_L = \frac{\triangle\,{}_0S[P^A_{x:\,m,\,n}]}{\triangle\,{}_0S[P^A_{x:\,m,\,n}] - \triangle\,{}_0S[P^L_{x:\,m,\,n}]}. \tag{4.1}$$

Since the NSP of discrete life insurance can be expressed in terms of the NSPs of annuities (for example, the NSPs of the discrete n-year endowment, the discrete whole life insurance and the discrete n-year term life insurance satisfy $A_{x:\,\overline{n}|} = 1 - d\cdot \ddot{a}_{x:\,\overline{n}|}$, $A_x = 1 - d\cdot\ddot{a}_x$ and $A^1_{x:\,\overline{n}|} = A_{x:\,\overline{n}|} - {}_nE_x = 1 - d\cdot\ddot{a}_{x:\,\overline{n}|} - {}_nE_x$, respectively, where $d = i/(1+i)$ is the discount rate), ${}_0S^*[P^L_{x:\,m,\,n}] = P^L_{x:\,m,\,n}\cdot \ddot{a}^*_{x:\,\overline{m}|} - A^*_{x,\,n}$ can be rewritten as ${}_0S^*[P^L_{x:\,m,\,n}] = \sum_{k=0}^n N^L_k \cdot {}_kp^*_x \cdot e^{-\delta\cdot k}$ for some $N^L_k, k = 0,1,\ldots,n$, where N^L_k, the net cash flow (cash inflow less cash outflow) at time k, can be positive, zero or negative. Similarly, ${}_0S[P^L_{x:\,m,\,n}] = \sum_{k=0}^n N^L_k \cdot {}_kp_x \cdot e^{-\delta\cdot k}$. Therefore, the change in ${}_0S[P^L_{x:\,m,\,n}]$ by (3.8) becomes

$$\triangle\,{}_0S[P^L_{x:\,m,\,n}] \triangleq {}_0S^*[P^L_{x:\,m,\,n}] - {}_0S[P^L_{x:\,m,\,n}] = \sum_{k=0}^n N^L_k \cdot \triangle\,{}_kp_x(U_{x,\,k})\cdot e^{-\delta\cdot k},$$

where $\triangle\,{}_kp_x(U_{x,\,k})$ is given by (3.5) or (3.7). Following the same argument, the change in ${}_0S[P^A_{x:\,m,\,n}]$ can be also re-written as

$$\triangle\,{}_0S[P^A_{x:\,m,\,n}] \triangleq {}_0S^*[P^A_{x:\,m,\,n}] - {}_0S[P^A_{x:\,m,\,n}] = \sum_{k=0}^n N^A_k \cdot \triangle\,{}_kp_x(U_{x,\,k})\cdot e^{-\delta\cdot k},$$

for some $N^A_k, k = 0,1,\ldots,n$. Thus, the weight $\hat{w}_L$ in (4.1) depends on α_k and/or β_k, $k = 1,2,\ldots,n$. Moreover, $\triangle\,{}_0S^{LA}_{x:\,m,\,n}$ can be re-written as

$$\triangle\,{}_0S^{LA}_{x:\,m,\,n} = \sum_{k=0}^n N^{LA}_k\cdot\triangle\,{}_kp_x(U_{x,\,k})\cdot e^{-\delta\cdot k} = \sum_{k=0}^n I^{LA}_k\cdot\triangle\,{}_kp_x(U_{x,\,k})\cdot e^{-\delta\cdot k} - \sum_{k=0}^n O^{LA}_k\cdot\triangle\,{}_kp_x(U_{x,\,k})\cdot e^{-\delta\cdot k}.$$

where $N^{LA}_k = w_L\cdot N^L_k + (1-w_L)\cdot N^A_k$, $N^{LA}_k = I^{LA}_k - O^{LA}_k$, and I^{LA}_k and O^{LA}_k are the cash inflow and cash outflow at time k in the portfolio, respectively. Therefore, $\triangle\,{}_0S^{LA}_{x:\,m,\,n} = 0$ means the present value of the changes in cash inflows match that in cash outflows.

The $\triangle\,{}_kp_x(U_{x,\,k})$ in each of $\triangle\,{}_0S[P^L_{x:\,m,\,n}]$ and $\triangle\,{}_0S[P^A_{x:\,m,\,n}]$ involves a remainder term for each k. We may ignore these remainder terms since both α_k and β_k are very small (see Figure 5.1) and the third order and higher of α_k and β_k are less than 10^{-5} and 10^{-11}, respectively. Depending on what assumption we make on $\triangle\, {}_kp_x(U_{x,\,k})$ in (3.7), there are several $\hat{w}_L$s can be obtained from (4.1). Denote $\hat{w}_L(M_n^\gamma)$ the weight of the life insurance product in an insurance portfolio using the matching strategy M_n^γ, where M can be D, C or DC indicating that the duration function, the convexity function or both the duration and convexity functions are included in $\triangle\, {}_kp_x(U_{x,\,k})$, respectively; γ can be p, c or pc indicating that the proportional relational model, the constant relational model or the linear relational model is adopted, respectively; n is the maximum length of the mortality sequences. The estimated weights are

- $\hat{w}_L(D_n^p)$: $\triangle\, {}_kp_x(U_{x,\,k}) \doteq {}_kp_x \cdot d_{U_{x,\,k}}^p \cdot \alpha_k$;
- $\hat{w}_L(D_n^c)$: $\triangle\, {}_kp_x(U_{x,\,k}) \doteq {}_kp_x \cdot d_{U_{x,\,k}}^c \cdot \beta_k$;
- $\hat{w}_L(D_n^{pc})$: $\triangle\, {}_kp_x(U_{x,\,k}) \doteq {}_kp_x \cdot [d_{U_{x,\,k}}^p \cdot \alpha_k + d_{U_{x,\,k}}^c \cdot \beta_k]$;
- $\hat{w}_L(C_n^p)$: $\triangle\, {}_kp_x(U_{x,\,k}) \doteq {}_kp_x \cdot c_{U_{x,\,k}}^p \cdot \alpha_k^2/2$;
- $\hat{w}_L(C_n^c)$: $\triangle\, {}_kp_x(U_{x,\,k}) \doteq {}_kp_x \cdot c_{U_{x,\,k}}^c \cdot \beta_k^2/2$;
- $\hat{w}_L(C_n^{pc})$: $\triangle\, {}_kp_x(U_{x,\,k}) \doteq {}_kp_x \cdot [c_{U_{x,\,k}}^p \cdot \alpha_k^2/2 + c_{U_{x,\,k}}^c \cdot \beta_k^2/2 + c_{U_{x,\,k}}^{p\,c} \cdot \alpha_k\beta_k]$;
- $\hat{w}_L(DC_n^p)$: $\triangle\, {}_kp_x(U_{x,\,k}) \doteq {}_kp_x \cdot [d_{U_{x,\,k}}^p \cdot \alpha_k + c_{U_{x,\,k}}^p \cdot \alpha_k^2/2]$;
- $\hat{w}_L(DC_n^c)$: $\triangle\, {}_kp_x(U_{x,\,k}) \doteq {}_kp_x \cdot [d_{U_{x,\,k}}^c \cdot \beta_k + c_{U_{x,\,k}}^c \cdot \beta_k^2/2]$; and
- $\hat{w}_L(DC_n^{cp})$: $\triangle\, {}_kp_x(U_{x,\,k}) \doteq {}_kp_x \cdot [d_{U_{x,\,k}}^p \cdot \alpha_k + d_{U_{x,\,k}}^c \cdot \beta_k + c_{U_{x,\,k}}^p \cdot \frac{\alpha_k^2}{2} + c_{U_{x,\,k}}^c \cdot \frac{\beta_k^2}{2} + c_{U_{x,\,k}}^{p\,c} \cdot \alpha_k\beta_k]$.

For $\hat{w}_L(D_n^p)$, $\hat{w}_L(D_n^c)$, $\hat{w}_L(C_n^p)$ and $\hat{w}_L(C_n^c)$, when $\alpha_k = \alpha$ and $\beta_k = \beta$ for $k = 1, 2, \ldots, n$, we can factor out the common α and β from both $\triangle\, {}_0S[P_{x:\,m,\,n}^L]$ and $\triangle\, {}_0S[P_{x:\,m,\,n}^A]$ and then cancel out α from $\hat{w}_L(D_n^p)$ and $\hat{w}_L(C_n^p)$, and β from $\hat{w}_L(D_n^c)$ and $\hat{w}_L(C_n^c)$. In this case, $\hat{w}_L(D_n^p)$, $\hat{w}_L(D_n^c)$, $\hat{w}_L(C_n^p)$ and $\hat{w}_L(C_n^c)$ become independent of α and β, and are re-denoted as $\hat{w}_L(D^p)$, $\hat{w}_L(D^c)$, $\hat{w}_L(C^p)$ and $\hat{w}_L(C^c)$, respectively, which are

$$\hat{w}_L(B^\lambda) = \frac{\sum_{k=0}^n N_k^A \cdot b_{U_{x,\,k}}^\lambda \cdot {}_kp_x \cdot e^{-\delta\cdot k}}{\sum_{k=0}^n N_k^A \cdot b_{U_{x,\,k}}^\lambda \cdot {}_kp_x \cdot e^{-\delta\cdot k} - \sum_{k=0}^n N_k^L \cdot b_{U_{x,\,k}}^\lambda \cdot {}_kp_x \cdot e^{-\delta\cdot k}},$$

where $\lambda = p$ (proportional), c (constant) and $(B,\, b) = (D,\, d)$ (duration), $(C,\, c)$ (convexity), as proposed in Tsai and Chung (2013) for $U = \mu$, in Lin and Tsai (2013) for $U = P$, Q and μ, and in Lin and Tsai (2014) for $U = P$, Q, μ, $\ln(\mu)$, Q/P and $\ln(Q/P)$.

For $\hat{w}_L(D_n^p)$, $\hat{w}_L(C_n^p)$ and $\hat{w}_L(DC_n^p)$ ($\hat{w}_L(D_n^c)$, $\hat{w}_L(C_n^c)$ and $\hat{w}_L(DC_n^c)$) involving only α_k (β_k), we use the proportional relational model $U_{x,\,k}^* = (1+\alpha_k)\cdot U_{x,\,k} + e_{x,k}$ (constant relational model $U_{x,\,k}^* = U_{x,\,k} + \beta_k + e_{x,k}$) to estimate α_k (β_k) for $k = 1, \ldots, n$; for $\hat{w}_L(D_n^{pc})$, $\hat{w}_L(C_n^{pc})$ and $\hat{w}_L(DC_n^{pc})$ involving α_k and β_k, we use the linear relational model $U_{x,\,k}^* = (1+\alpha_k)\cdot U_{x,\,k} + \beta_k + e_{x,k}$ to estimate α_k and β_k for $k = 1, \ldots, n$. The estimates of α_k and β_k are obtained by minimizing the sum of squared errors. For the proportional relational model, the estimate is

$$\hat{\alpha}_k = \frac{\sum_{j=1}^{k} u_{x+j-1} \cdot (u^*_{x+j-1} - u_{x+j-1})}{\sum_{j=1}^{k} u^2_{x+j-1}}; \tag{4.2}$$

for the constant relational model, the estimate is

$$\hat{\beta}_k = \bar{u}^*_{x,\,k} - \bar{u}_{x,\,k}, \tag{4.3}$$

where u^*_{x+j-1} and u_{x+j-1} are the $x+j-1$ element in $U^*_{x,\,k}$ and $U_{x,\,k}$, respectively; $\bar{u}^*_{x,\,k} = (1/k)\sum_{j=1}^{k} u^*_{x+j-1}$ and $\bar{u}_{x,\,k} = (1/k)\sum_{j=1}^{k} u_{x+j-1}$; for the linear relational model, the estimates are

$$(\hat{\alpha}_k,\, \hat{\beta}_k) = \Big(\frac{\sum_{j=1}^{k}[u_{x+j-1} - \bar{u}_{x,\,k}] \cdot [u^*_{x+j-1} - \bar{u}^*_{x,\,k}]}{\sum_{j=1}^{k}[u_{x+j-1} - \bar{u}_{x,\,k}]^2} - 1,\, \bar{u}^*_{x,\,k} - [1+\hat{\alpha}_k] \cdot \bar{u}_{x,\,k}\Big). \tag{4.4}$$

Theorem 1.. *For $U = \mu = -\ln P$,*
(a) $\hat{w}_L(D^{p\,c}_n) = \hat{w}_L(D^c_n)$,
(b) $\hat{w}_L(C^{p\,c}_n) = \hat{w}_L(C^c_n)$, and
(c) $\hat{w}_L(DC^{p\,c}_n) = \hat{w}_L(DC^c_n)$.

Proof: If $U = \mu = -\ln(P)$, we have $\bar{u}^*_{x,\,k} = (1/k)\sum_{j=1}^{k}[-\ln(p^*_{x+j-1})] = -(1/k)\ln({}_kp^*_x)$ and $\bar{u}_{x,\,k} = -(1/k)\ln({}_kp_x)$; moreover, $d^p_{\mu_{x,\,k}} = \ln({}_kp_x)$, $d^c_{\mu_{x,\,k}} = -k$, $c^p_{\mu_{x,\,k}} = [\ln({}_kp_x)]^2$ and $c^c_{\mu_{x,\,k}} = k^2$ from Tables 2 and 3.

(a) For $\hat{w}_L(D^c_n)$, $\hat{\beta}_k = \bar{u}^*_{x,\,k} - \bar{u}_{x,\,k} = -[\ln({}_kp^*_x) - \ln({}_kp_x)]/k$ by (4.3), and $\triangle\,{}_kp_x(\mu_{x,\,k}) \doteq {}_kp_x \cdot d^c_{\mu_{x,\,k}} \cdot \hat{\beta}_k = {}_kp_x \cdot [\ln({}_kp^*_x) - \ln({}_kp_x)]$, $k = 1, \ldots, n$. For $\hat{w}_L(D^{p\,c}_n)$, $\hat{\beta}_k = \bar{u}^*_{x,\,k} - [1+\hat{\alpha}_k] \cdot \bar{u}_{x,\,k} = -\ln({}_kp^*_x)/k + (1+\hat{\alpha}_k) \cdot \ln({}_kp_x)/k$ by (4.4), and $\triangle\,{}_kp_x[\mu_{x,\,k}] \doteq {}_kp_x \cdot [d^p_{\mu_{x,\,k}} \cdot \hat{\alpha}_k + d^c_{\mu_{x,\,k}} \cdot \hat{\beta}_k]$ becomes

$${}_kp_x \cdot [\ln({}_kp_x) \cdot \hat{\alpha}_k - k \cdot \hat{\beta}_k] = {}_kp_x \cdot [\ln({}_kp_x) \cdot \hat{\alpha}_k + \ln({}_kp^*_x) - [1+\hat{\alpha}_k] \cdot \ln({}_kp_x)] = {}_kp_x \cdot [\ln({}_kp^*_x) - \ln({}_kp_x)],$$

the $\triangle\,{}_kp_x[\mu_{x,\,k}]$ for $\hat{w}_L(D^c_n)$. Thus, $\hat{w}_L(D^{p\,c}_n) = \hat{w}_L(D^c_n)$.

(b) For $\hat{w}_L(C^c_n)$, $\triangle\,{}_kp_x[\mu_{x,\,k}] \doteq {}_kp_x \cdot c^c_{\mu_{x,\,k}} \cdot \hat{\beta}^2_k/2 = {}_kp_x \cdot [\ln({}_kp^*_x) - \ln({}_kp_x)]^2/2$. For $\hat{w}_L(C^{p\,c}_n)$, $\triangle\,{}_kp_x[\mu_{x,\,k}] \doteq {}_kp_x \cdot [c^p_{\mu_{x,\,k}} \cdot \hat{\alpha}^2_k/2 + c^c_{\mu_{x,\,k}} \cdot \hat{\beta}^2_k/2 + d^p_{\mu_{x,\,k}}\, d^c_{\mu_{x,\,k}} \cdot \hat{\alpha}_k\hat{\beta}_k]$ is

$$\begin{aligned} &{}_kp_x \cdot \Big\{[\ln({}_kp_x)]^2 \cdot \frac{\hat{\alpha}^2_k}{2} + k^2 \cdot \frac{[-\ln({}_kp^*_x) + (1+\hat{\alpha}_k) \cdot \ln({}_kp_x)]^2}{2\,k^2} \\ &+(-k)\,[\ln({}_kp_x)] \cdot \hat{\alpha}_k \frac{-\ln({}_kp^*_x) + (1+\hat{\alpha}_k) \cdot \ln({}_kp_x)}{k}\Big\} = {}_kp_x \cdot \frac{[\ln({}_kp^*_x) - \ln({}_kp_x)]^2}{2}, \end{aligned}$$

the $\triangle\,{}_kp_x(\mu_{x,\,k})$ for $\hat{w}_L(C^c_n)$. Hence, $\hat{w}_L(C^{p\,c}_n) = \hat{w}_L(C^c_n)$.

(c) For $\hat{w}_L(DC_n^c)$, $\triangle\, {}_kp_x(\mu_{x,k}) \doteq {}_kp_x \cdot [d^c_{\mu_{x,k}} \cdot \hat{\beta}_k + c^c_{\mu_{x,k}} \cdot \hat{\beta}_k^2/2] = {}_kp_x \cdot [\ln({}_kp_x^*) - \ln({}_kp_x)] + {}_kp_x \cdot [\ln({}_kp_x^*) - \ln({}_kp_x)]^2/2$, the sum of $\triangle\, {}_kp_x(\mu_{x,k})$s for $\hat{w}_L(D_n^c)$ and $\hat{w}_L(C_n^c)$, which is also the sum of $\triangle\, {}_kp_x(\mu_{x,k})$s for $\hat{w}_L(D_n^{pc})$ and $\hat{w}_L(C_n^{pc})$ by (b) and (c). Therefore, $\hat{w}_L(DC_n^{pc}) = \hat{w}_L(DC_n^c)$. $\square$

4.2 Two insurance portfolios

In this project, we focus on two types of insurance portfolios,

- PFL^{TP}: the m-payment and n-year term life insurance and the m-payment and n-year pure endowment with weights w_{TL} and $1 - w_{TL}$, respectively, and
- PFL^{WA}: the m-payment whole life insurance and the m-payment and n-year deferred whole life annuity with weights w_{WL} and $1 - w_{WL}$, respectively.

When the experienced force of mortality is different from the predetermined one, the change in the surpluses of term life insurance and pure endowment, $\Delta\, {}_0S[P^{TL}_{x:\,m,n}]$ and $\Delta\, {}_0S[P^{PE}_{x:\,m,n}]$, respectively, are

$$\begin{aligned}\Delta\, {}_0S[P^{TL}_{x:\,m,n}] &= P^{TL}_{x:\,m,n}\Delta\ddot{a}_{x:\,\overline{m}|}(U_{x,n}) - \Delta A^{1}_{x:\,\overline{n}|}(U_{x,n}) \\ &= P^{TL}_{x:\,m,n}\Delta\ddot{a}_{x:\,\overline{m}|}(U_{x,n}) + d \cdot \Delta\ddot{a}_{x:\,\overline{n}|}(U_{x,n}) + \Delta\, {}_n|\ddot{a}_{x:\,\overline{1}|}(U_{x,n}),\end{aligned} \tag{4.5}$$

and

$$\begin{aligned}\Delta\, {}_0S[P^{PE}_{x:\,m,n}] &= P^{PE}_{x:\,m,n}\Delta\ddot{a}_{x:\,\overline{m}|}(U_{x,n}) - \Delta\, {}_nE_x(U_{x,n}) \\ &= P^{PE}_{x:\,m,n}\Delta\ddot{a}_{x:\,\overline{m}|}(U_{x,n}) - \Delta\, {}_n|\ddot{a}_{x:\,\overline{1}|}(U_{x,n}),\end{aligned} \tag{4.6}$$

where $P^{TL}_{x:\,m,n}$ is the net level premium of the m-payment and n-year term life insurance and $P^{TL}_{x:\,m,n} = A^{1}_{x:\,\overline{n}|}/\ddot{a}_{x:\,\overline{m}|} = (1 - d\ddot{a}_{x:\,\overline{n}|} - {}_nE_x)/\ddot{a}_{x:\,\overline{m}|}$; $P^{PE}_{x:\,m,n}$ is the net level premium of the m-payment and n-year pure endowment and $P^{PE}_{x:\,m,n} = {}_nE_x/\ddot{a}_{x:\,\overline{m}|} = {}_n|\ddot{a}_{x:\,\overline{1}|}/\ddot{a}_{x:\,\overline{m}|}$. Since the net level premiums $P^{TL}_{x:\,m,n}$ and $P^{PE}_{x:\,m,n}$ are calculated using the predicted mortality rates before the policies are issued, the premiums are not affected by the future mortality movements. In addition, the change in the portfolio surplus is

$$\begin{aligned}\Delta\, {}_0S^{TP} &= w_{TL} \cdot \Delta\, {}_0S[P^{TL}_{x:\,m,n}] + (1 - w_{TL}) \cdot \Delta\, {}_0S[P^{PE}_{x:\,m,n}] \\ &= w_{TL} \cdot \sum_{k=0}^{n} N_k^{TL} \cdot \triangle\, {}_kp_x(U_{x,k}) \cdot e^{-\delta\cdot k} + (1 - w_{TL}) \cdot \sum_{k=0}^{n} N_k^{PE} \cdot \triangle\, {}_kp_x(U_{x,k}) \cdot e^{-\delta\cdot k},\end{aligned} \tag{4.7}$$

where

$$
\begin{aligned}
N_k^{TL} &= P_{x:m,n}^{TL} + d,\ k = 0, \ldots, m-1,\ m \geq 1, \\
N_k^{TL} &= d,\ k = m, \ldots, n-1,\ m \leq n, \text{ and} \\
N_n^{TL} &= 1
\end{aligned}
$$

by (4.5), and

$$
\begin{aligned}
N_k^{PE} &= P_{x:m,n}^{PE},\ k = 0, \ldots, m-1,\ m \geq 1, \\
N_k^{PE} &= 0,\ k = m, \ldots, n-1,\ m \leq n, \text{ and} \\
N_n^{PE} &= -1
\end{aligned}
$$

by (4.6). Depending on the assumption we make on $\triangle\, {}_k p_x(U_{x,k})$ in (3.7), we can obtain different estimates for $\Delta\, {}_0 S[P_{x:m,n}^{PE}]$, $\Delta\, {}_0 S[P_{x:m,n}^{TL}]$ under different strategies. Then we can further determine the corresponding weight for each matching strategy according to (4.1).

Similarly, when the experienced force of mortality is different from the predetermined one, the change in the surpluses of whole life insurance and deferred annuity products, $\Delta\, {}_0 S[P_{x:m,n}^{WL}]$ and $\Delta\, {}_0 S[P_{x:m,n}^{DA}]$, respectively, are

$$
\begin{aligned}
\Delta\, {}_0 S[P_{x:m,n}^{WL}] &= P_{x:m,n}^{WL} \Delta \ddot{a}_{x:\overline{m}|}(U_{x,\omega-x}) - \Delta A_x(U_{x,\omega-x}) \\
&= P_{x:m,n}^{WL} \Delta \ddot{a}_{x:\overline{m}|}(U_{x,\omega-x}) + d \cdot \Delta \ddot{a}_x(U_{x,\omega-x}),
\end{aligned}
\tag{4.8}
$$

and

$$
\Delta\, {}_0 S[P_{x:m,n}^{DA}] = P_{x:m,n}^{DA} \Delta \ddot{a}_{x:\overline{m}|} - \Delta\, {}_n|\ddot{a}_x, \tag{4.9}
$$

where ω is the limiting age that no one attained, $P_{x:m,n}^{WL}$ is the net level premium of the m-payment whole life insurance and $P_{x:m,n}^{WL} = A_x/\ddot{a}_{x:\overline{m}|} = (1 - d\ddot{a}_x)/\ddot{a}_{x:\overline{m}|}$; $P_{x:m,n}^{DA}$ is the net level premium of the m-payment and n-year deferred whole life annuity and $P_{x:m,n}^{DA} = {}_n|\ddot{a}_x/\ddot{a}_{x:\overline{m}|}$. Since the net level premiums $P_{x:m,n}^{WL}$ and $P_{x:m,n}^{DA}$ are calculated using the predicted mortality rates before the policies are issued, the premiums are not affected by the future mortality movements. In addition, the change in the portfolio surplus is

$$\begin{aligned}\Delta_0 S^{WA} &= w_{WL}\cdot\,\Delta_0 S[P^{WL}_{x:\,m,n}] + (1-w_{WL})\cdot\,\Delta_0 S[P^{DA}_{x:\,m,n}]\\ &= w_{WL}\cdot\sum_{k=0}^{\omega-x-1} N_k^{WL}\cdot\triangle_k p_x(U_{x,\,k})\cdot e^{-\delta\cdot k} + (1-w_{WL})\cdot\sum_{k=0}^{\omega-x-1} N_k^{DA}\cdot\triangle_k p_x(U_{x,\,k})\cdot e^{-\delta\cdot k},\end{aligned} \tag{4.10}$$

where, from (4.8) and (4.9),

$$\begin{aligned} N_k^{WL} &= P^{WL}_{x:\,m,n} + d,\; k = 0,\ldots,m-1,\; m\ge 1 and\\ N_k^{WL} &= d,\; k = m,\ldots,\omega - x\end{aligned}$$

and

$$\begin{aligned} N_k^{DA} &= P^{DA}_{x:\,m,n},\; k = 0,\ldots,m-1,\; 1\le m\le n,\\ N_k^{DA} &= 0,\; k = m,\ldots,n-1, and\\ N_k^{DA} &= -1,\; k = n,\ldots,\omega-x-1.\end{aligned}$$

Depending on the assumption on $\triangle_k p_x(U_{x,\,k})$ in (3.7), we can obtain different estimates for $\Delta_0 S[P^{DA}_{x:\,m,n}]$ and $\Delta_0 S[P^{WL}_{x:\,m,n}]$ and the corresponding estimates for weights according to (4.1).

4.3 Simulation procedure for surpluses

We calculate $\triangle_0 S[P^{L}_{x:\,m,\,n}]$ and $\triangle_0 S[P^{A}_{x:\,m,\,n}]$ for $\hat{w}_L$ with the following steps:

- (S1) forecast a mortality rate sequence of length n, $U_{x,\,n} = \{u_{x+j-1} : j = 1,\ldots,n\}$, where $\{u_{x+j-1}$ is the $j-th$ element in the diagonal of the deterministic Lee-Carter model;
- (S2) use the forecasted mortality sequence to calculate premiums $P^{L}_{x:\,m,\,n}$ and $P^{A}_{x:\,m,\,n}$;
- (S3) simulate N mortality sequences of length n, $U^{*,\,i}_{x,\,n} = \{u^{*,\,i}_{x+j-1} : j = 1,\ldots,n\}$, $i = 1,\ldots,N$, from the stochastic Lee-Carter model;
- (S4) fit $U^{*,\,i}_{x,\,k}$ with $U_{x,\,k}$ to obtain $\hat{\alpha}^i_k$ (proportional relational model) by (4.2), $\hat{\beta}^i_k$ (constant relational model) by (4.3), and $(\hat{\alpha}^i_k,\, \hat{\beta}^i_k)$ (linear relational model) by (4.4) for $k = 1,\ldots,n$ and $i = 1,\ldots,N$, and compute $\bar{\hat{\alpha}}_k$, $\bar{\hat{\beta}}_k$ and $(\bar{\hat{\alpha}}_k,\, \bar{\hat{\beta}}_k)$ where $\bar{\hat{\alpha}}_k = (1/N)\sum_{i=1}^N \hat{\alpha}^i_k$ and $\bar{\hat{\beta}}_k = (1/N)\sum_{i=1}^N \hat{\beta}^i_k$ for $k = 1,\ldots,n$;
- (S4*) fit $\bar{U}^{*}_{x,\,k}$ with $U_{x,\,k}$ to obtain $\bar{\hat{\alpha}}_k$ (proportional relational model) by (4.2), $\bar{\hat{\beta}}_k$ (constant relational model) by (4.3), and $(\bar{\hat{\alpha}}_k,\, \bar{\hat{\beta}}_k)$ (linear relational model) by (4.4) where $\bar{U}^{*}_{x,\,k} = (1/N)\sum_{i=1}^N U^{*,\,i}_{x,\,k}$ for $k = 1,\ldots,n$;

- (S5) use $\bar{\hat{\alpha}}_k$, $\bar{\hat{\beta}}_k$ and $(\bar{\hat{\alpha}}_k, \bar{\hat{\beta}}_k)$, $k = 1, \ldots, n$, to calculate $\triangle\, {}_k p_x(U_{x,k})$s based on different assumptions, which are then plugged into $(\triangle\, {}_0 S[P^L_{x:\,m,\,n}], \triangle\, {}_0 S[P^A_{x:\,m,\,n}])$ to obtain corresponding $\hat{w}_L$ by (4.1);

- (S6) calculate the i^{th} weighted surplus ${}_0S^{i,LA}_{x:\,m,\,n} = \hat{w}_L \cdot {}_0S^i[P^L_{x:\,m,\,n}] + (1-\hat{w}_L)\cdot {}_0S^i[P^A_{x:\,m,\,n}]$ at time zero based on the i^{th} mortality sequence, $i = 1, \ldots, N$.

Note that Steps (S4*) and (S4) are equivalent in producing $\bar{\hat{\alpha}}_k$, $\bar{\hat{\beta}}_k$ and $(\bar{\hat{\alpha}}_k, \bar{\hat{\beta}}_k)$, $k = 1, \ldots, n$, since by (4.2)

$$\begin{aligned}
\bar{\hat{\alpha}}_k &= \frac{\sum_{j=1}^k u_{x+j-1}\cdot(\bar{u}^*_{x+j-1} - u_{x+j-1})}{\sum_{j=1}^k u^2_{x+j-1}} = \frac{\sum_{j=1}^k u_{x+j-1}\cdot\frac{1}{N}\sum_{i=1}^N (u^{*,\,i}_{x+j-1} - u_{x+j-1})}{\sum_{j=1}^k u^2_{x+j-1}} \\
&= \frac{1}{N}\sum_{i=1}^N \frac{\sum_{j=1}^k u_{x+j-1}(u^{*,\,i}_{x+j-1} - u_{x+j-1})}{\sum_{j=1}^k u^2_{x+j-1}} = \frac{1}{N}\sum_{i=1}^N \hat{\alpha}^i_k, \qquad (4.11)
\end{aligned}$$

by (4.3)

$$\begin{aligned}
\bar{\hat{\beta}}_k &= \frac{1}{k}\sum_{j=1}^k (\bar{u}^*_{x+j-1} - u_{x+j-1}) = \frac{1}{k}\sum_{j=1}^k \frac{1}{N}\sum_{i=1}^N (u^{*,\,i}_{x+j-1} - u_{x+j-1}) \\
&= \frac{1}{N}\sum_{i=1}^N \frac{1}{k}\sum_{j=1}^k (u^{*,\,i}_{x+j-1} - u_{x+j-1}) = \frac{1}{N}\sum_{i=1}^N (\bar{u}^{*,\,i}_{x+j-1} - \bar{u}_{x+j-1}) = \frac{1}{N}\sum_{i=1}^N \hat{\beta}^i_k, \qquad (4.12)
\end{aligned}$$

and by (4.4)

$$\begin{aligned}
\bar{\hat{\alpha}}_k &= \frac{\sum_{j=1}^k (u_{x+j-1} - \bar{u}_{x,\,k})\cdot\frac{1}{N}\sum_{i=1}^N (u^{*,\,i}_{x+j-1} - \bar{u}^{*,\,i}_{x,\,k})}{\sum_{j=1}^k (u_{x+j-1} - \bar{u}_{x,\,k})^2} - 1 \\
&= \frac{1}{N}\sum_{i=1}^N \Big[\frac{\sum_{j=1}^k (u_{x+j-1} - \bar{u}_{x,\,k})\cdot(u^{*,\,i}_{x+j-1} - \bar{u}^{*,\,i}_{x,\,k})}{\sum_{j=1}^k (u_{x+j-1} - \bar{u}_{x,\,k})^2} - 1\Big] = \frac{1}{N}\sum_{i=1}^N \hat{\alpha}^i_k \qquad (4.13)
\end{aligned}$$

and

$$\bar{\hat{\beta}}_k = \frac{1}{N}\sum_{i=1}^N \bar{u}^{*,\,i}_{x,\,k} - (1+\hat{\alpha}_k)\cdot\bar{u}_{x,\,k} = \frac{1}{N}\sum_{i=1}^N [\bar{u}^{*,\,i}_{x,\,k} - (1+\hat{\alpha}^i_k)\cdot\bar{u}_{x,\,k}] = \frac{1}{N}\sum_{i=1}^N \hat{\beta}^i_k. \qquad (4.14)$$

Therefore, we adopt Step (S4*) because it requires less computational effort.

Chapter 5

Numerical illustrations

In this chapter, we review the findings in Lin and Tsai (2014) and decide to set U to μ for the numerical illustrations in this project. Then we exhibit that the coefficients $\hat{\alpha}_k$s, $\hat{\beta}_k$s and $(\hat{\alpha}_k, \hat{\beta}_k)$s of the proportional, constant and linear relational models, respectively, with $\mu^*_{x,k}$ and $\mu_{x,k}$ being used as the realized and expected cohort forces of mortality are varying by k. We also compare the hedge performances of size free and non-size free matching strategies for the following insurance portfolios issued to the cohort aged x in 2011:

- ${}_{20}PFL^{TP}$: a portfolio of 20-payment and 20-year term life insurance and 20-payment and 20-year pure endowment;
- ${}_{65-x}PFL^{TP}$: a portfolio of (65-x)-payment and (65-x)-year term life insurance and (65-x)-payment and (65-x)-year pure endowment;
- ${}_{20}PFL^{WA}$: a portfolio of 20-payment whole life insurance and 20-payment and 20-year deferred whole life annuity;
- ${}_{65-x}PFL^{WA}$: a portfolio of (65-x)-payment whole life insurance and (65-x)-payment and (65-x)-year deferred whole life annuity.

According to Theorem 1, $\hat{w}_L(D_n^{pc}) = \hat{w}_L(D_n^c)$ and $\hat{w}_L(C_n^{pc}) = \hat{w}_L(C_n^c)$ when U is set to the force of mortality μ. As a result, the size free and non-size free matching strategies are paired for comparisons as follows:

Table 4. *Pairing size free and non-size free matching strategies*

Size free	*Non-size free*
D^p	D_n^p
D^c	D_n^c (D_n^{pc})
C^p	C_n^p
C^c	C_n^c (C_n^{pc})

The numerical results shown in this chapter are based on the USA male mortality rates under the Lee-Carter model described in Chapter 3. The deterministic forecasted mortality path is used as the pricing path $\mu_{x,n}$, while the mean of 10,000 stochastic forecasted mortality paths is used as the realized path $\mu^*_{x,n}$ to obtain the estimates of α_ks, β_ks and $(\alpha_k, \beta_k)s$ with formulas defined in Chapter 4. The weights of products in each insurance portfolio are determined by the assumptions on $\Delta\,_k p_x$ made in Chapter 4. In addition, we simulate another set of 10,000 stochastic forecasted mortality paths to find the risk quantities: variance, value at risk (VaR) and conditional tail expectation (CTE), for illustrating hedging performances. We use 2% as the interest rate for discounting cashflows.

5.1 A review

Lin and Tsai (2014) studied the cases that U can take μ, Q, P, Q/P, $\ln \mu$ and $\ln Q/P$, proposed twenty-four size free matching strategies with respect to an instantaneous proportional or constant change in U, and classified them into seven groups according to the weights calculated. In each group, all members result in weights close to each other, which will lead to similar hedging performances. Members of each group are listed below (see Lin and Tsai, 2014).

Table 5. *Members of groups by the matching strategies*

Duration groups	*Members*
G_{D1}	$D^p(\mu_x),\ D^p(Q_x),\ D^c(\ln(\mu_x)),\ D^p(Q_x/P_x),\ D^c(\ln(Q_x/P_x))$
G_{D2}	$D^p(\ln(\mu_x)),\ D^p(\ln(Q_x/P_x))$
G_{D3}	$D^c(\mu_x),\ D^c(Q_x),\ D^p(P_x),\ D^c(P_x),\ D^c(Q_x/P_x)$
Convexity groups	*Members*
G_{C1}	$C^p(\mu_x),\ C^p(Q_x),\ C^p(Q_x/P_x)$
G_{C2}	$C^c(\mu_x),\ C^c(Q_x),\ C^p(P_x),\ C^c(P_x),\ C^c(Q_x/P_x)$
G_{C3}	$C^c(\ln(\mu_x)),\ C^c(\ln(Q_x/P_x))$
G_{C4}	$C^p(\ln(\mu_x)),\ C^p(\ln(Q_x/P_x))$

Lin and Tsai (2014) omited G_{C3} and G_{C4} because these two groups might result in negative weights for PFL^{TP} and PFL^{WA} portfolios. In the second stage, Lin and Tsai (2014) chose $D^p(\mu_x)$, $D^p(\ln(\mu_x))$, $D^c(\mu_x)$, $C^p(\mu_x)$ and $C^c(\mu_x)$ as the representatives of the groups G_{D1}, G_{D2}, G_{D3}, G_{C1} and G_{C2}, respectively. According to their findings, they suggested $D^p(\mu_x)$, $D^c(\mu_x)$, $C^p(\mu_x)$ and $C^c(\mu_x)$ as the final four candidates for further comparisons. In order to compare the hedging performance of non-size free strategies with that of size free ones, we focus on the case of $U = \mu$ in this project. In addition, we use the deterministic cohort mortality sequence $\mu_{x,n} = \{\mu_{x,t_0}, \ldots, \mu_{x+n-1,t_0+n-1}\}$ for pricing and the simulated cohort mortality sequence $\mu^*_{x,n} = \{\mu^*_{x,t_0}, \ldots, \mu^*_{x+n-1,t_0+n-1}\}$ for realization of the surplus where t_0 is 2011, the first prediction year in our project. Then the linear relational model becomes

$$\mu^*_{x,\,k} - \mu_{x,\,k} = \alpha_k \times \mu_{x,\,k} + \beta_k + e_{x,k},\ k = 1, \ldots, n. \tag{5.1}$$

5.2 Estimation for $\alpha_k\, s$ and $\beta_k\, s$

The estimates of the proportional and constant shift parameters, $\hat{\alpha}_k$ and $\hat{\beta}_k$, can be obtained using the expected mortality rate sequence of length k for $\mu_{x,k}$ and the simulated one for $\mu^*_{x,k}$ by the least squares linear regression method specified in (4.11), (4.12), and (4.13) and (4.14) for the proportional, constant and linear relational models, respectively. Figures 5.1 and 5.2 show the 10 estimated sequences of $\hat{\alpha}_k$s, $\hat{\beta}_k$s and $(\hat{\alpha}_k, \hat{\beta}_k)$s by fitting $\bar{\mu}^*_{x,k}$, the average of 10,000 stochastically simulated mortality rate sequences, with $\mu_{x,k}$, the expected mortality rate sequence (see Step S4* in the simulation for surpluses in Section 4.3), 10 times for the cohorts currently aged 25 and 45, respectively. Since we not only assume both proportional and constant shifts but also proportional or constant movement only, we have four subplots in each figure accordingly. From those figures, we can verify that $\hat{\alpha}_k$s, $\hat{\beta}_k$s and $(\hat{\alpha}_k, \hat{\beta}_k)$s vary by k, where k is the length of the sequences $\mu_{x,k}$ and $\bar{\mu}^*_{x,k}$ used in fitting. Therefore, developing non-size free matching strategies rather than size free matching strategies is reasonable. Moreover, from the figures for the two different ages, we can conclude the following in terms of stability:

- When $k = 1$, the linear relational model is fitted as the constant relational model, therefore $\hat{\alpha}_1 = 0$;
- No matter which of the linear, proportional and constant relational models we apply, the estimates $(\hat{\alpha}_k, \hat{\beta}_k)$, $\hat{\alpha}_k$ only, or $\hat{\beta}_k$ only for the young age cohort are more stable than the mid-age cohort;
- In general, the estimates from the proportional or constant relational model assuming proportional or constant shift only ($\hat{\alpha}_k$ only or $\hat{\beta}_k$ only) are more stable than those from the linear relational model with both proportional and constant shifts $(\hat{\alpha}_k, \hat{\beta}_k)$, especially when k is small.

From the aspect of achieving relatively high stability, we tend to use the strategies based on either proportional or constant shift instead of those based on both proportional and constant shifts. According to Theorem 1, the weights obtained from D_n^{pc} and C_n^{pc} are the same as the ones from D_n^c and C_n^c, respectively; we hence do not consider the linear relational model in the following illustrations.

Figure 5.1: Estimates of α_k and/or β_k for age 25

(a) $\hat{\alpha}_k$ from the linear relational model

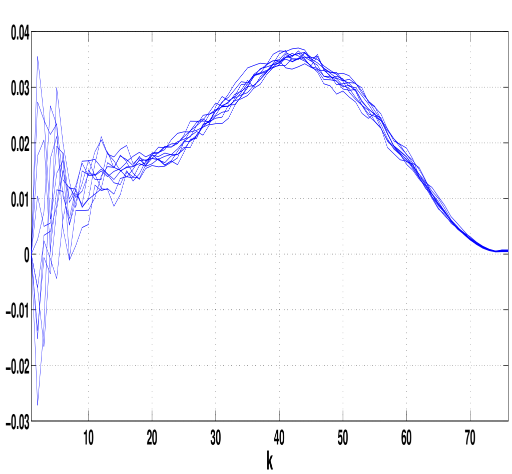

(b) $\hat{\beta}_k$ from the linear relational model

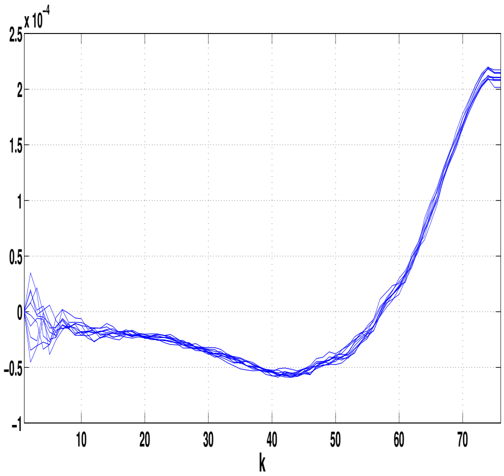

(c) $\hat{\alpha}_k$ from the proportional relational model

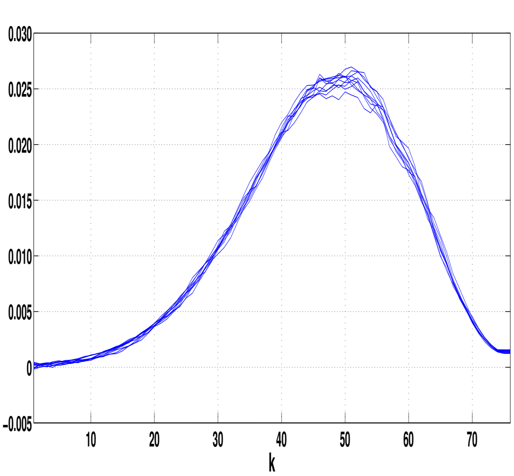

(d) $\hat{\beta}_k$ from the constant relational model

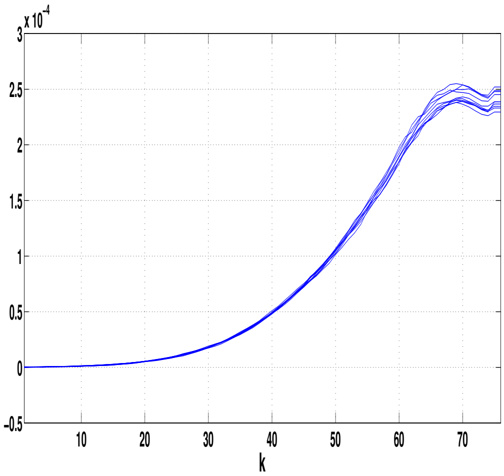

Figure 5.2: Estimates of α_k and/or β_k for age 45

(a) $\hat{\alpha}_k$ from the linear relational model

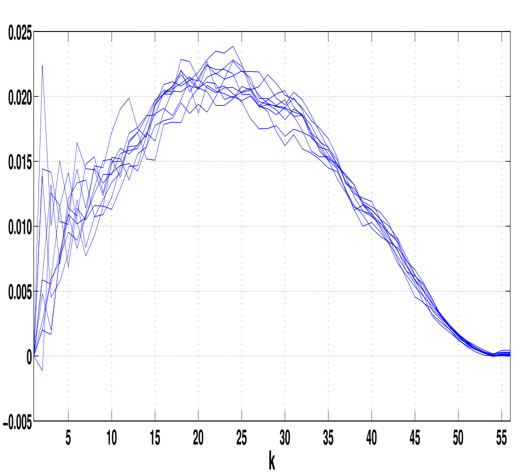

(b) $\hat{\beta}_k$ from the linear relational model

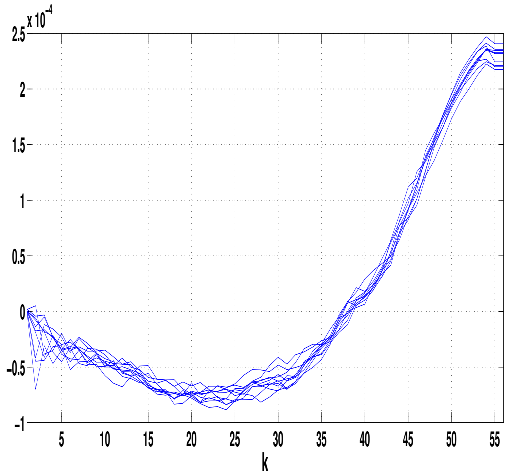

(c) $\hat{\alpha_k}$ from the proportional relational model

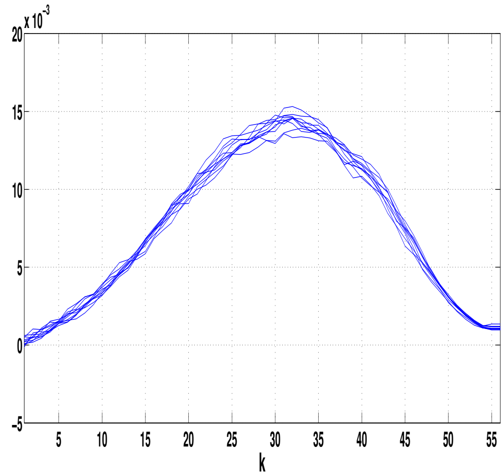

(d) $\hat{\beta_k}$ from the constant relational model

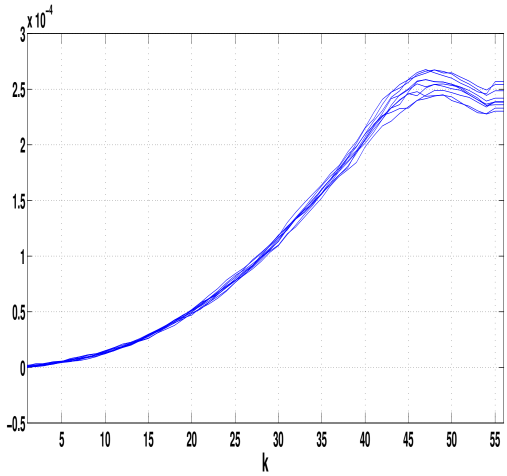

5.3 Hedging performance at time 0

In this section we compare the hedge performances of size free and non-size free strategies for the four insurance portfolios, ${}_{20}PFL^{TP}$, ${}_{65-x}PFL^{TP}$, ${}_{20}PFL^{WA}$ and ${}_{65-x}PFL^{WA}$. We first compare hedge effectiveness for mortality and longevity risks in Subsection 5.3.1, and then compare hedge performances using value at risk (VaR) and conditional tail expectation (CTE) in Subsection 5.3.2.

5.3.1 Hedge effectiveness

Two insurance portfolios are created to hedge against both mortality and longevity risks. We achieve the goal of hedging with various weights of two products in the portfolios, where the weights are determined according to different matching strategies. Denote ${}_0S^L$, ${}_0S^A$ and ${}_0S^P$ the simulated surpluses at time 0 for life insurance, annuity and the portfolio, respectively. Hedge effectiveness (HE) is the variance reduction ratio indicating the degree of the variability of the portfolio less than the variance of the surplus of a single product in the portfolio (Li and Hardy, 2011). The closer the hedge effectiveness is to 100%, the more effective the hedging strategy is. The hedge effectiveness for mortality risk (HE^m) and longevity risk (HE^l) are defined as follows:

$$HE^m(\sigma^2) = \frac{\sigma^2({}_0S^L) - \sigma^2({}_0S^P)}{\sigma^2({}_0S^L)} = 1 - \frac{\sigma^2({}_0S^P)}{\sigma^2({}_0S^L)}, \tag{5.2}$$

and

$$HE^l(\sigma^2) = \frac{\sigma^2({}_0S^A) - \sigma^2({}_0S^P)}{\sigma^2({}_0S^A)} = 1 - \frac{\sigma^2({}_0S^P)}{\sigma^2({}_0S^A)}. \tag{5.3}$$

We assumed that the ${}_{20}PFL^{TP}$ and ${}_{20}PFL^{WA}$ portfolios are issued to insureds aged from 20 to 80, while the ${}_{65-x}PFL^{TP}$ and ${}_{65-x}PFL^{WA}$ portfolios are issued to insured aged from 20 to 60. For each portfolio, we first demonstrate the one-by-one comparisons of hedge effectiveness for mortality and longevity risks against age x between size free and non-size free matching strategies, and then select top two candidates from each of the size free and non-size free groups of matching strategies for an overall comparison.

5.3.1.1 $_{20}$PFL portfolios

Since the hedge effectiveness for longevity risks of the $_{20}PFL^{TP}$ and $_{20}PFL^{WA}$ portfolios decrease dramatically to negative values for age beyond 70, we only show the HEs for longevity risk up to age 70 for those two portfolios. We summarize the results from Figures 5.3 to 5.6 as follows:

- The $HE(\sigma^2)$s for mortality risk for $_{20}PFL^{TP}$ are above 90% for all eight candidates for all ages from 20 to 80, while the $HE(\sigma^2)$s for longevity risk remain high (above 85%) for ages from 20 to 60, and then drop dramatically. The $HE(\sigma^2)$s for mortality risk for $_{20}PFL^{WA}$ have a left skewed hyperbolic shape; all candidates except for D^c start above 95% and remain above 80% for ages from 20 to 40, and then they start decreasing and reach the troughs below 50% around age 65; the $HE(\sigma^2)$s fall below zero for D^c for ages from 32 to 72 and for D_n^p for ages from 64 to 69. The negative $HE(\sigma^2)$s indicate that the mortality risk becomes more intensive by creating such portfolio than the original life insurance product. Similar to portfolio $_{20}PFL^{TP}$, the $HE(\sigma^2)$s for longevity risk for $_{20}PFL^{WA}$ remain high (above 99%) for ages from 20 to 60, and then decrease dramatically.

- From (a) and (b) in Figure 5.3, the comparison between matching strategies D^p and D_n^p for $_{20}PFL^{TP}$ shows that D_n^p is more preferable because it improves the HEs for D^p up to 3% and 5% for mortality and longevity risks, respectively. Although the $HE(\sigma^2)$s for D_n^p strategy are lower than those for D^p strategy for some ages, the differences are less than 0.5% for mortality risk and 2% for longevity risk. For $_{20}PFL^{WA}$ portfolio, the $HE(\sigma^2)$s for D_n^p are higher than those for D^p from age 20 to age 57 with a maximum difference about 5%, but it goes below D^p from age 58 to age 75 with a trough below 0. From (b) in Figure 5.4 for longevity risk, it is hard to tell whether D_n^p is more effective than D^p from ages 20 to 60 because those two lines lie together, whereas it is obvious that the non-size free strategy D_n^p is less effective than the D^p strategy.

- From (c) and (d) in Figures 5.3 and 5.4, we can see that the non-size free strategy D_n^c is more effective than the size free strategy D^c for both $_{20}PFL^{TP}$ and $_{20}PFL^{WA}$ portfolios. Furthermore, the non-size free strategy D_n^c for mortality risk improves $HE(\sigma^2)$ over 5% and 250% at some ages for the $_{20}PFL^{TP}$ and $_{20}PFL^{WA}$ portfolios, respectively.

- From (e) and (f) in Figure 5.3 for the $_{20}PFL^{TP}$ portfolio, the advantage of using non-size free strategy C_n^p is obvious for ages beyond 65; the maximum difference in $HE(\sigma^2)$ between C_n^p and C^p for mortality risk is around 3.5%. From (e) and (f) in Figure 5.4 for the $_{20}PFL^{WA}$ portfolio, the advantage of using non-size free strategy C_n^p is obvious for ages beyond 55 for mortality risk; the maximum difference in $HE(\sigma^2)$ between C_n^p and C^p for mortality risk is around 12%. Although we can see that C_n^p lies above C^p in the longevity graph for ages beyond 66, the difference is less than 3%.

- From (g) and (h) in Figure 5.3 for the ${}_{20}PFL^{TP}$ portfolio, the non-size free strategy C_n^c improves $HE(\sigma^2)$ up to 1.5% for ages from 20 to 68 for both mortality and longevity risks. However, for ages from 69 to 76 the C_n^c strategy is less effective than the C^c one. From (g) in Figure 5.4 for the ${}_{20}PFL^{WA}$ portfolio, the non-size free strategy C_n^c shows a larger improvement in hedge effectiveness for mortality risk from ages 20 to 69; the maximum difference in $HE(\sigma^2)$ between C_n^c and C^c is 20%. However, from (h) in Figure 5.4 it is hard to differentiate the performance of C_n^c from that of C^c for ages from 20 to 55 for longevity risk.

- From (a) and (b) in Figure 5.5 for the ${}_{20}PFL^{TP}$ portfolio, we pick C^p and C^c as top two candidates from the size free matching strategy group. From (c) and (d) in Figure 5.5, we pick C_n^p and C_n^c as top two candidates from the non-size free matching strategy group. From the overall comparison between the top four candidates from the size free and non-size free matching groups, we recommend the non-size free matching strategy with respect to proportional changes, C_n^p, whose performance is compatible with C^p strategy from age 20 to 65 and better than the C^p strategy for ages beyond 65. Moreover, the performance of the non-size free matching strategy with respect to constant changes, C_n^c, is also better than the C^p strategy and very close to the C_n^p strategy.

- From (a) and (b) in Figure 5.6 for the ${}_{20}PFL^{WA}$ portfolio, we take C^p and D^p as top two candidates from the size free matching strategy group. From (c) and (d) in Figure 5.6, we take C_n^p and C_n^c as top two candidates from the non-size free matching strategy group. From the overall comparison between the top four candidates from the size free and non-size free matching groups, we also recommend the non-size free matching strategy with respect to proportional changes, C_n^p, which performs the best over all ages and incorporate the advantage of both C^p and D^p. Furthermore, the hedge effectiveness of C_n^p and C_n^c strategies are close to each other.

- The non-size free matching strategy with respect to proportional changes, C_n^p, is the best candidate among all eight size free/non-size free matching strategies. Furthermore, the conclusion drawn from the $HE(\sigma^2)$s for mortality and longevity risks agree with each other.

Figure 5.3: Hedge effectiveness HE(σ^2) for ${}_{20}PFL^{TP}$ (I)

mortality risk (left column) | longevity risk (right column)

(a) D^p v.s. D^p_n

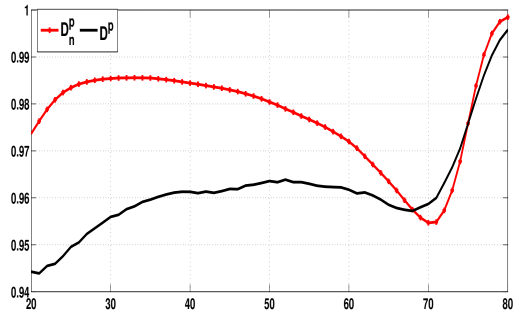

(b) D^p v.s. D^p_n

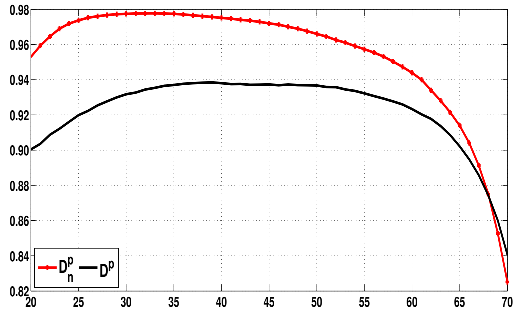

(c) D^c v.s. D^c_n

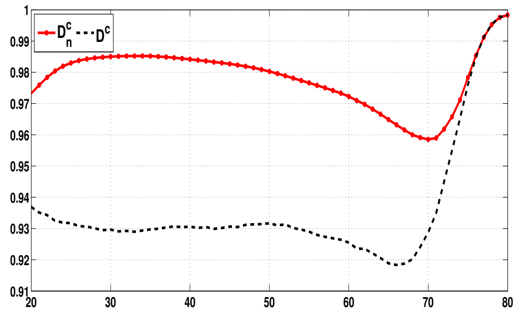

(d) D^c v.s. D^c_n

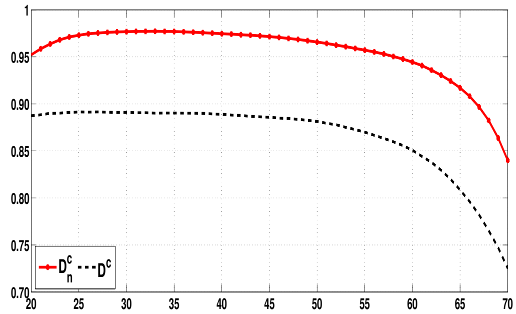

(e) C^p v.s. C^p_n

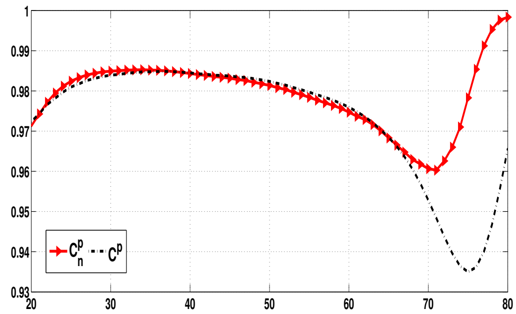

(f) C^p v.s. C^p_n

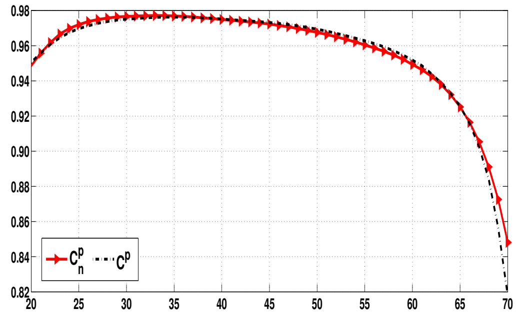

(g) C^c v.s. C^c_n

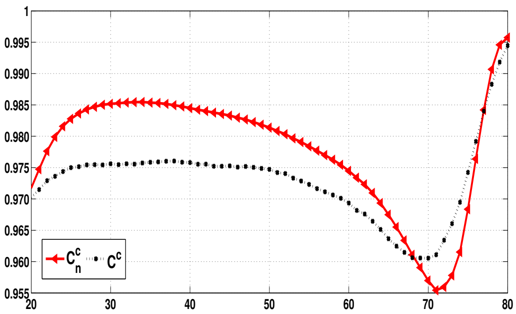

(h) C^c v.s. C^c_n

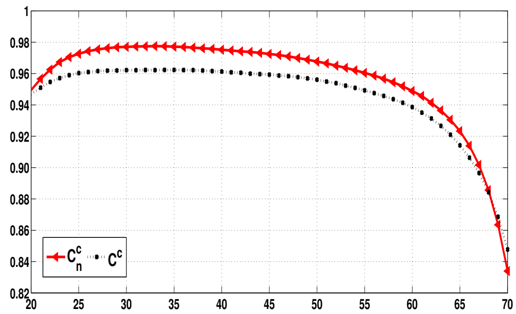

Figure 5.4: Hedge effectiveness HE(σ^2) for ${}_{20}PFL^{WA}$ (I)

mortality risk (left column) | longevity risk (right column)

(a) D^p v.s. D_n^p

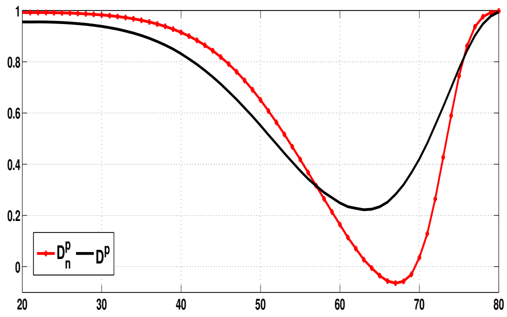

(b) D^p v.s. D_n^p

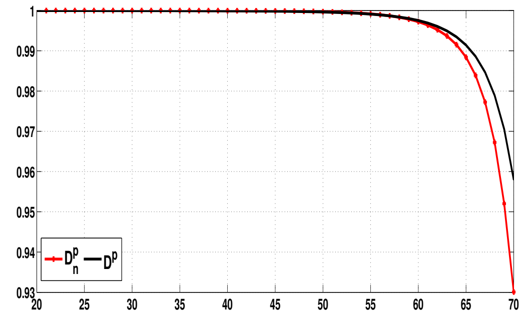

(c) D^c v.s. D_n^c

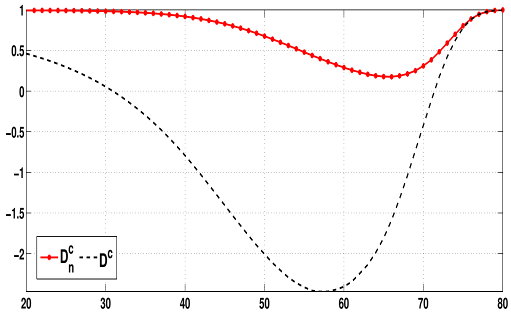

(d) D^c v.s. D_n^c

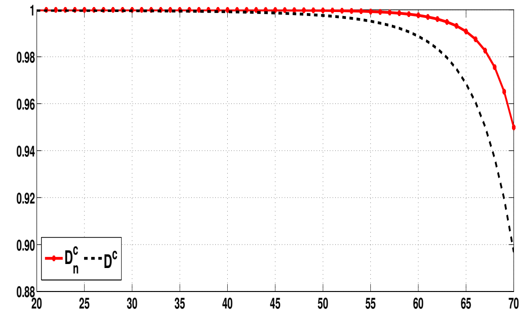

(e) C^p v.s. C_n^p

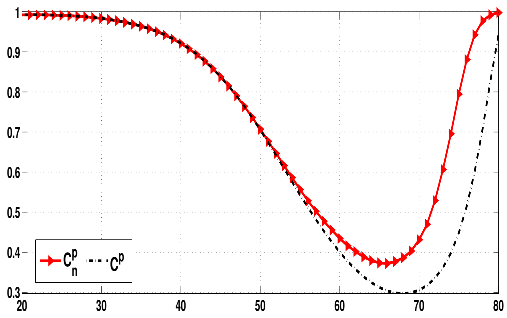

(f) C^p v.s. C_n^p

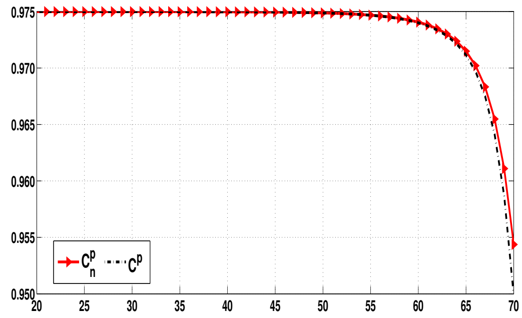

(g) C^c v.s. C_n^c

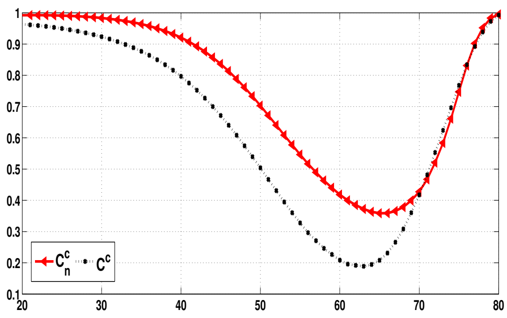

(h) C^c v.s. C_n^c

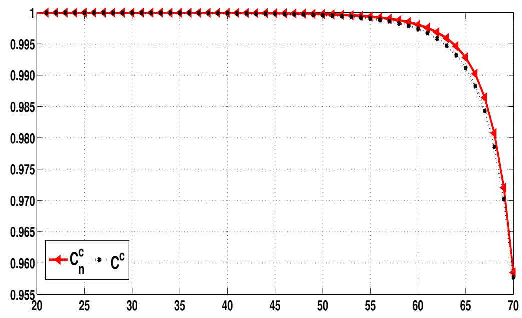

Figure 5.5: Hedge effectiveness HE(σ^2) for ${}_{20}PFL^{TP}$ (II)

mortality risk (left column) longevity risk (right column)

(a) size free strategies

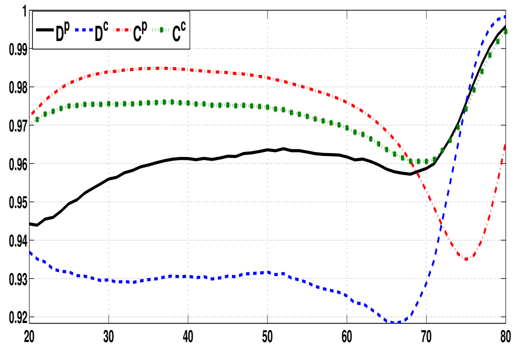

(b) size free strategies

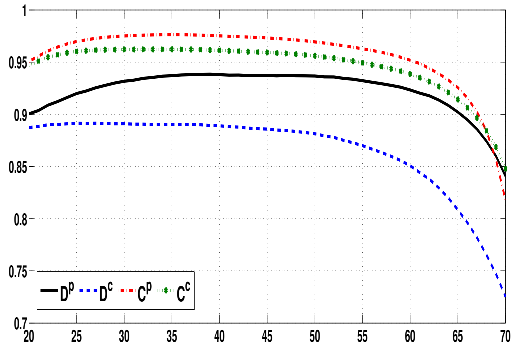

(c) non-size free strategies

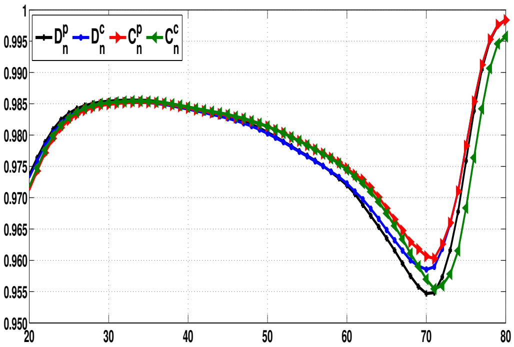

(d) non-size free strategies

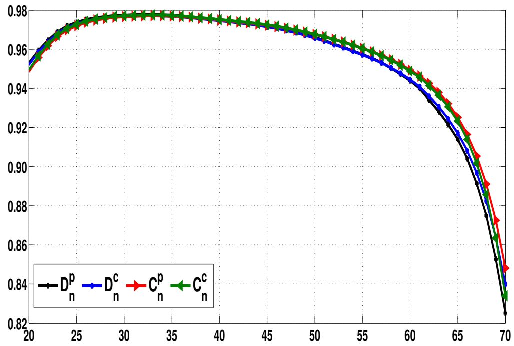

(e) size free v.s. non-size free

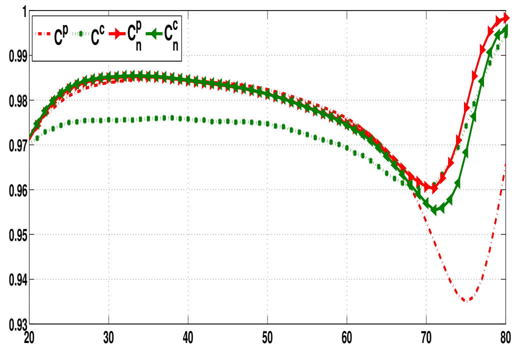

(f) size free v.s. non-size free

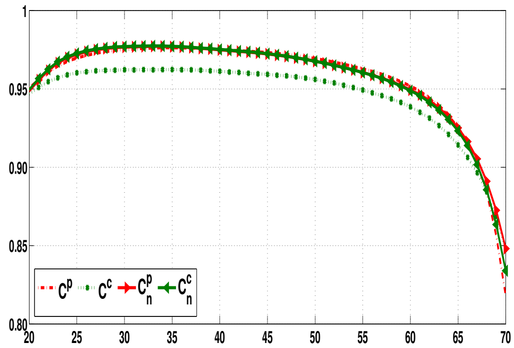

Figure 5.6: Hedge effectiveness HE(σ^2) for ${}_{20}PFL^{WA}$ (II)

mortality risk (left column) | longevity risk (right column)

(a) size free strategies

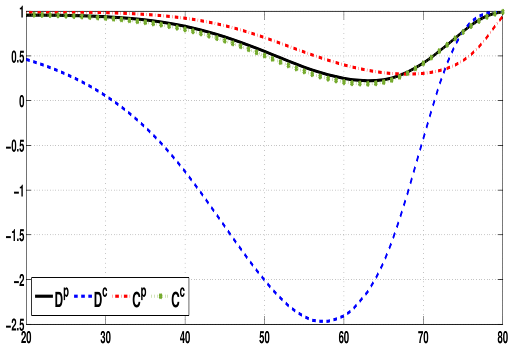

(b) size free strategies

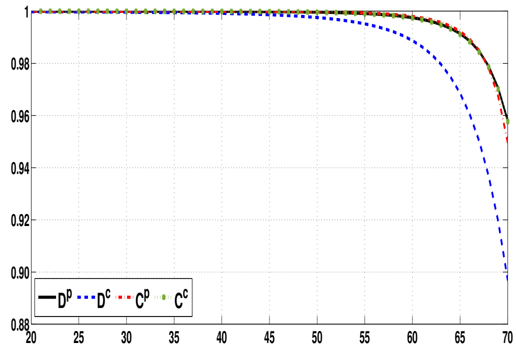

(c) non-size free strategies

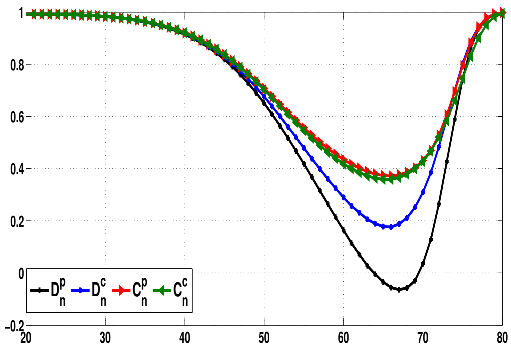

(d) non-size free strategies

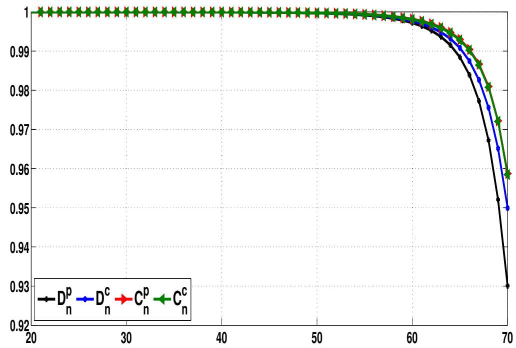

(e) size free v.s. non-size free

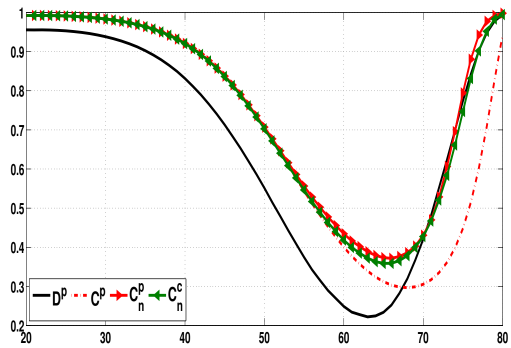

(f) (size free v.s. non-size free

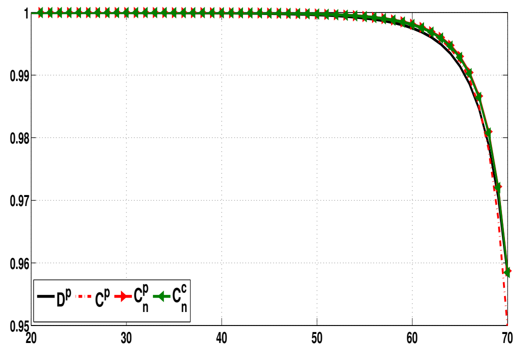

5.3.1.2 $_{65-x}$PFL portfolios

A summary of the $HE(\sigma^2)$s from Figures 5.7 to 5.10 for the portfolios $_{65-x}PFL^{TP}$ and $_{65-x}PFL^{WA}$ are given as follows:

- Subfigures (a) and (b) in Figures 5.7 and 5.8 illustrate that the D_n^p strategy has better performance than the D^p strategy for all ages. The improvements in hedge effectiveness for mortality and longevity risks are diminishing along ages for both portfolios. For the $_{65-x}PFL^{TP}$ portfolio, the differences between D_n^p and D^c are ranging from 1.1% to 3.8% for mortality risk and from 1.8% to 6% for longevity risk. For the $_{65-x}PFL^{WA}$ portfolio, the differences between D_n^p and D^c are ranging from 3.5% to 21.5% for mortality risk and from 0.001% to 0.012% for longevity risk. Because the variation of such life insurance product is relatively small comparing to the annuity product and a significant weight is put on life insurance product, the mortality risk is more sensitive to the weight changes than the longevity ones. Therefore, the improvements by the non-size free strategies are so much more on mortality risk than on longevity risk.

- Similarly, subfigures (c) and (d) in Figures 5.7 and 5.8 show that the D_n^c strategy has better performance than the D^c strategy for all ages. The improvements in hedge effectiveness for mortality and longevity risks are also diminishing along ages for both portfolios. For the $_{65-x}PFL^{TP}$ portfolio, the differences between D_n^c and D^c are ranging from 1.5% to 12% for mortality risk and from 2.5% to 17% for longevity risk. For the $_{65-x}PFL^{WA}$ portfolio, the $HE(\sigma^2)$s for D_n^c are positive for all ages from 20 to 60 for mortality risk, while the $HE(\sigma^2)$s for D^c are negative for ages from 20 to 54.

- From (e) and (f) in Figure 5.7, we can see that the $HE(\sigma^2)$s for the C_n^p strategy are a little higher than the C^p ones from age 20 to 32, but the situation reverses beyond age 33. From (e) and (f) in Figure 5.8, it is hard to differentiate C_n^p from C^p because they are too close.

- Subfigures (g) and (h) in Figures 5.7 and 5.8 demonstrate that the $HE(\sigma^2)$s for the C_n^c strategy are generally higher than the C^c ones except for ages 57-60 for the $_{65-x}PFL^{TP}$ portfolio. The improvements in hedge effectiveness also decrease in age. Subfigures (g) in Figures 5.7 and 5.8 show the maximum difference in $HE(\sigma^2)$s between C_n^c and C^c are about 3.2% and 115% for the portfolios $_{65-x}PFL^{TP}$ and $_{65-x}PFL^{WA}$, respectively.

- From (a) and (b) in Figure 5.9 for the $_{65-x}PFL^{TP}$ portfolio, we pick C^p and C^c as top two candidates from the size free matching strategy group. From (c) and (d) in Figure 5.9, the performances of C_n^p and C_n^c are close to those of D_n^p and D_n^c. For consistency with those for the portfolio $_{20}PFL^{TP}$, we select C_n^p and C_n^c as the candidates for further comparisons. From the overall comparisons among the top candidates from the size free and non-size free matching strategy groups, we recommend the non-size free matching strategy for proportional changes, C_n^p, for only young ages from 20 to 32. The hedge effectiveness for the size free matching strategy with respect to proportional change, C^p, is compatible with or a little higher than that for the C_n^p for the ages beyond 32.

- From (a) and (b) in Figure 5.10 for the ${}_{65-x}PFL^{WA}$ portfolio, we take C^p and D^p as top two candidates from the size free matching strategy group. From (c) and (d) in Figure 5.10, we take the C_n^p and C_n^c as top two candidates from the non-size free matching strategy group. From the overall comparisons among the top candidates from the size free and non-size free matching strategy groups, we can hardly differentiate between the C_n^p and C^p matching strategies by the performance.

- From the overall comparisons for the ${}_{65-x}PFL^{TP}$ and ${}_{65-x}PFL^{WA}$ portfolios, we only recommend the non-size free matching strategy C_n^p for some young ages for the ${}_{65-x}PFL^{TP}$ portfolios; otherwise, the size free matching strategy C^p is more preferable to the non-size free matching strategy due to its simplicity and that they have similar performances.

Figure 5.7: Hedge effectiveness HE(σ^2) for ${}_{65-x}PFL^{TP}$ (I)

mortality risk (left column)

longevity risk (right column)

(a) D^p v.s. D^p_n

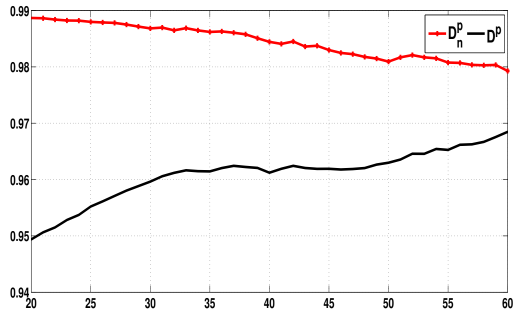

(b) D^p v.s. D^p_n

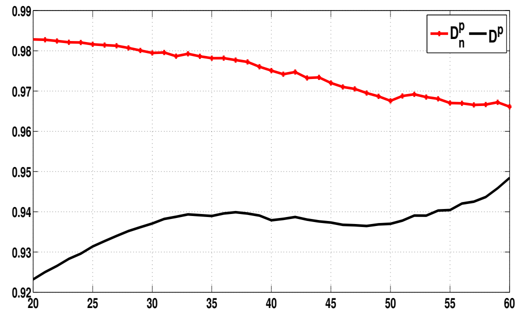

(c) D^c v.s. D^c_n

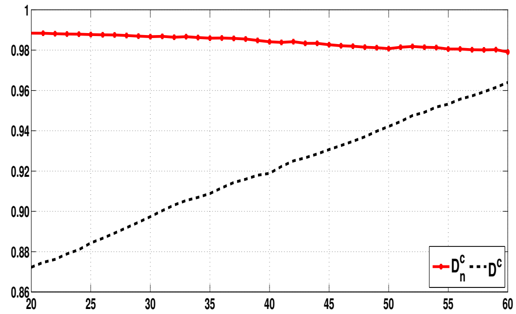

(d) D^c v.s. D^c_n

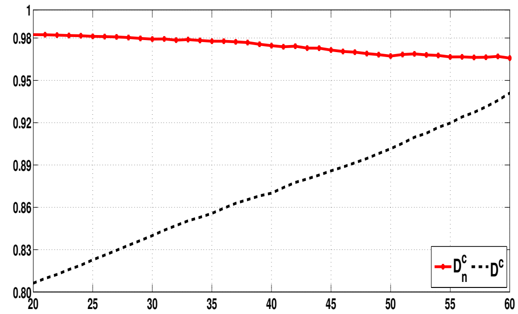

(e) C^p v.s. C^p_n

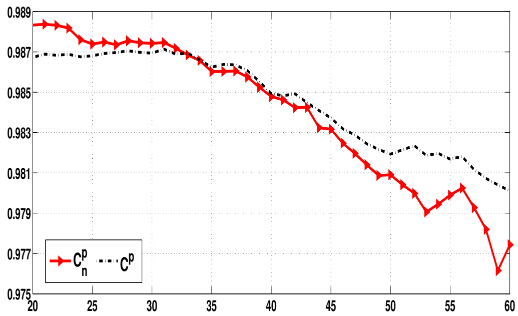

(f) C^p v.s. C^p_n

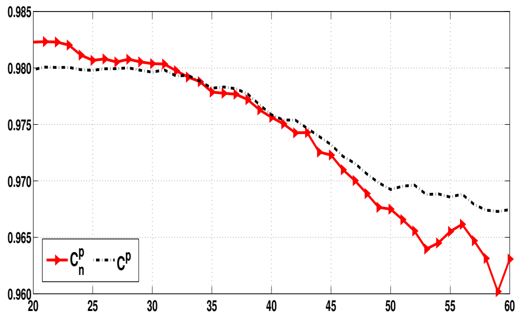

(g) C^c v.s. C^c_n

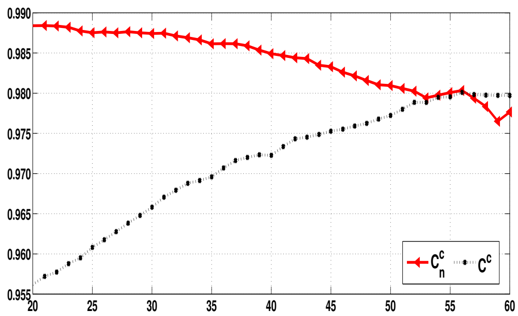

(h) C^c v.s. C^c_n

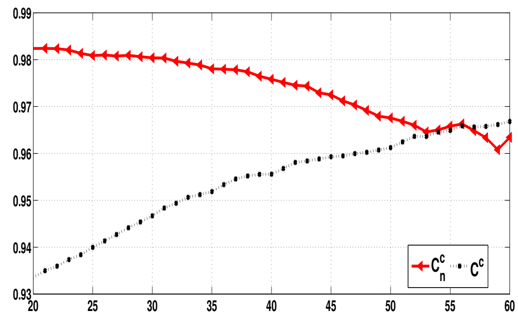

Figure 5.8: Hedge effectiveness HE(σ^2) for ${}_{65-x}PFL^{WA}$ (I)

mortality risk (left column)

(a) D^p v.s. D^p_n

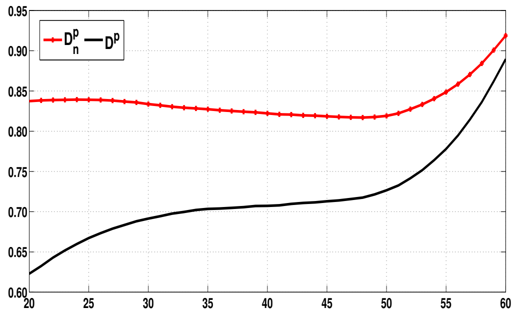

longevity risk (right column)

(b) D^p v.s. D^p_n

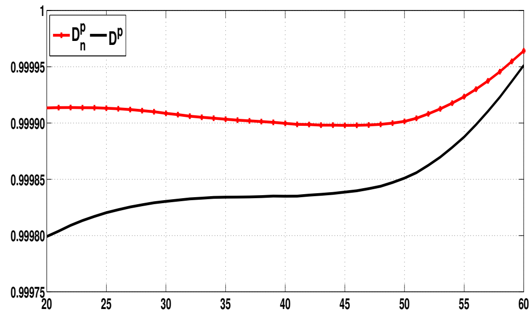

(c) D^c v.s. D^c_n

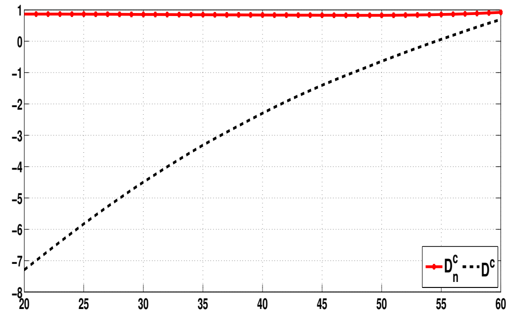

(d) D^c v.s. D^c_n

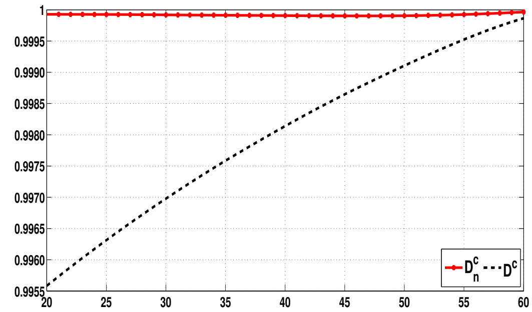

(e) C^p v.s. C^p_n

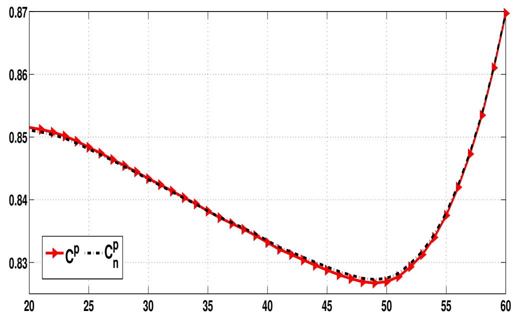

(f) C^p v.s. C^p_n

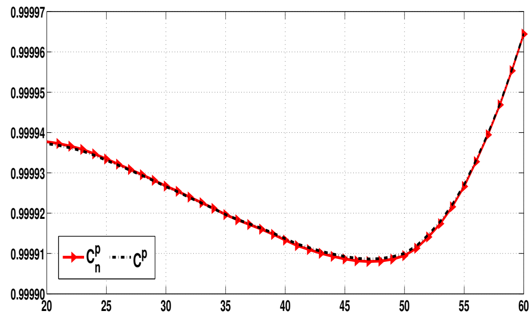

(g) C^c v.s. C^c_n

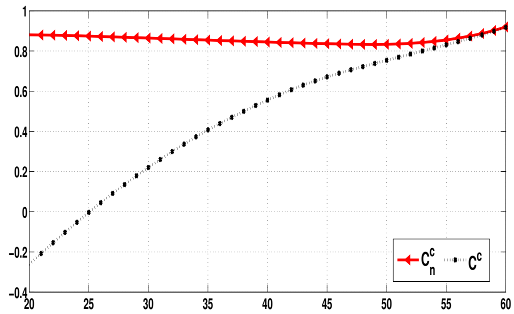

(h) C^c v.s. C^c_n

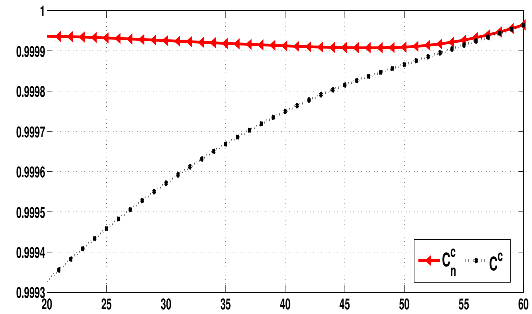

Figure 5.9: Hedge effectiveness HE(σ^2) for ${}_{65-x}PFL^{TP}$ (II)

mortality risk (left column) longevity risk (right column)

(a) size free strategies

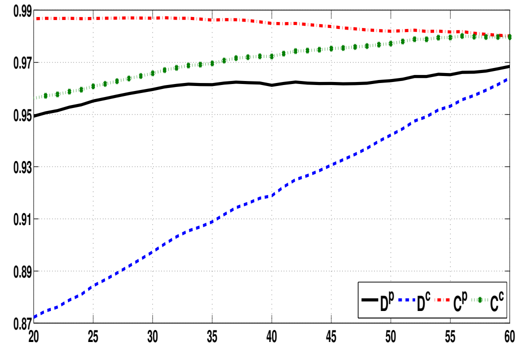

(b) size free strategies

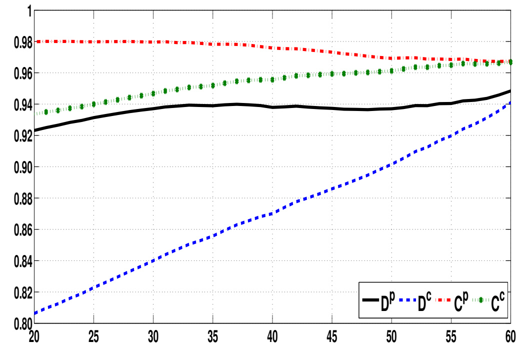

(c) non-size free strategies

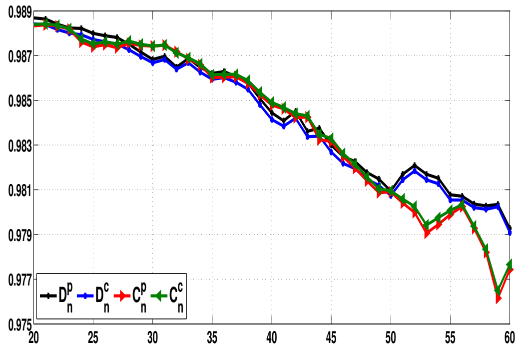

(d) non-size free strategies

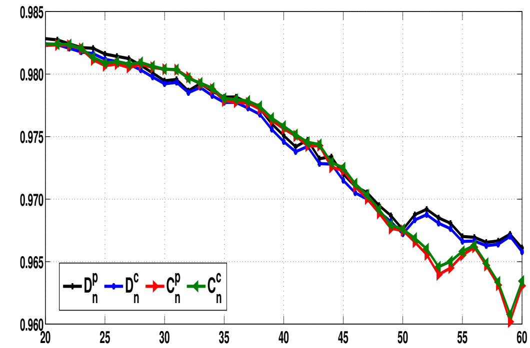

(e) size free v.s. non-size free

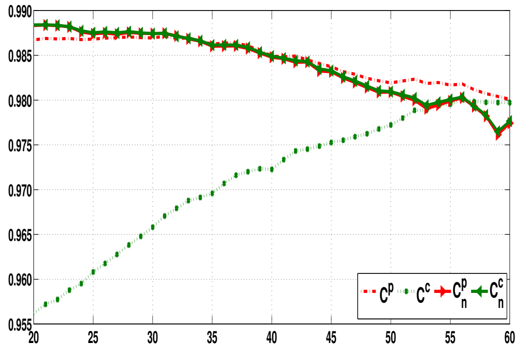

(f) size free v.s. non-size free

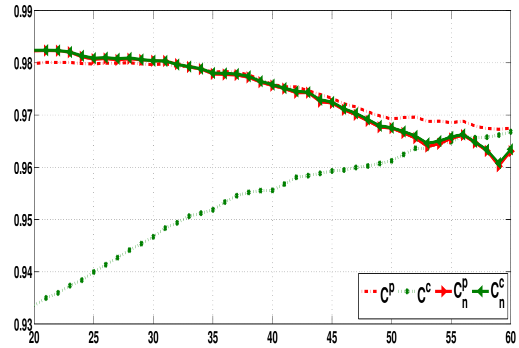

Figure 5.10: Hedge effectiveness HE(σ^2) for ${}_{65-x}PFL^{WA}$ (II)

mortality risk (left column) — longevity risk (right column)

(a) size free strategies

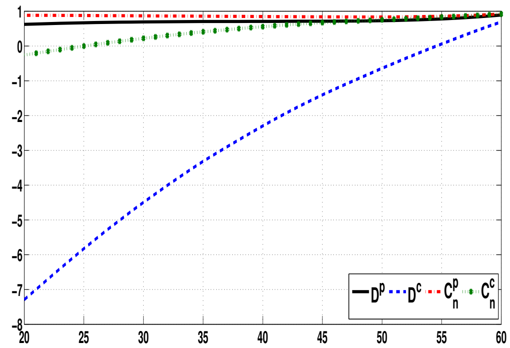

(b) size free strategies

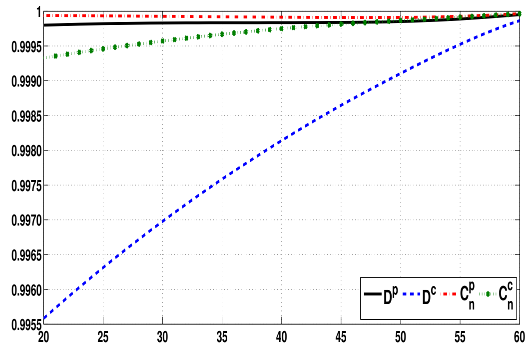

(c) non-size free strategies

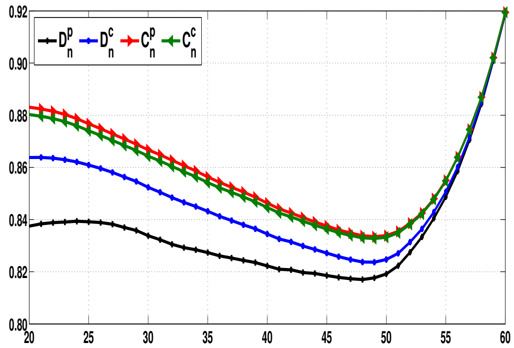

(d) non-size free strategies

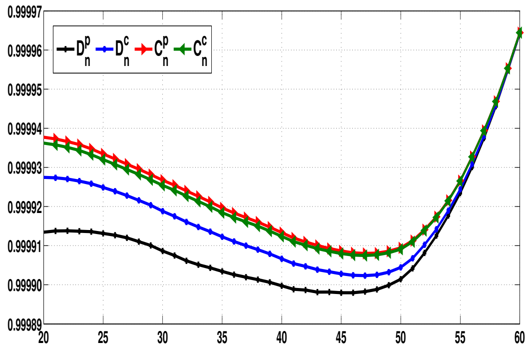

(e) size free v.s. non-size free

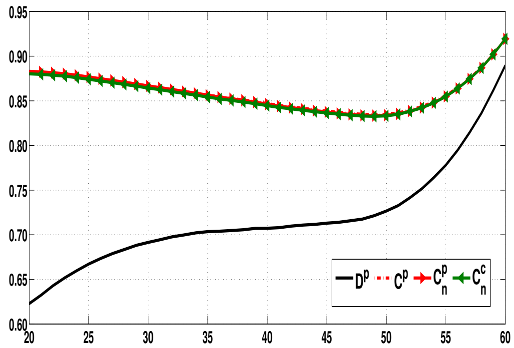

(f) size free v.s. non-size free

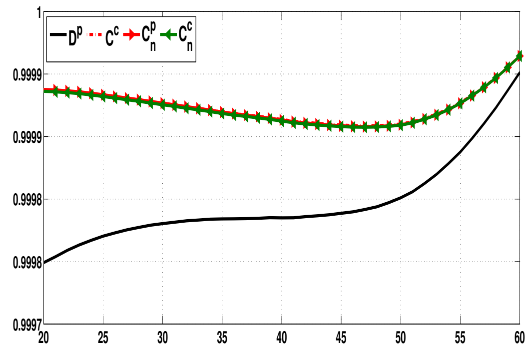

5.3.2 Other risk measures

Value at risk (VaR) and conditional tail expectation (CTE) are other important risk measure quantities widely used in finance, which report the value of extreme losses; for our case, γ-VaR is the negative γ-percentile of the simulated surpluses (Hull, 2012) and γ-CTE is the absolute value of the expectation of simulated surpluses given that the surplus is below the γ-percentile of the simulated surpluses. Because of the fact that a positive surplus value represents a gain while a negative surplus value stands for a loss, we desire both negative risk measure quantities γ-VaR and γ-CTE of the surplus to be as small as possible. For consistency with the four candidates in the preceding subsection, we select C^p, C^c, C_n^p and C_n^c for the portfolios ${}_{20}PFL^{TP}$ and ${}_{65-x}PFL^{TP}$, and D^p, C^p, C_n^p and C_n^c for the portfolios ${}_{20}PFL^{WA}$ and ${}_{65-x}PFL^{WA}$. A summary of observations from Figure 5.11 are given as follows:

- Paying attention to the scale of the vertical axis, 10^{-3} or 10^{-4}, we observe that the VaR and CTE of the portfolio surpluses are very small.
- From subfigures (a), (b), (e) and (f) for the ${}_{20}PFL^{TP}$ and ${}_{65-x}PFL^{TP}$ portfolios, we can see that although the C_n^p matching strategy doesn't result in the smallest VaR (CTE) for all ages 20 to 80, its value is very close to the smallest one among the other three selected matching strategies.
- From subfigures (c), (d), (g) and (h) for the ${}_{20}PFL^{WA}$ and ${}_{65-x}PFL^{WA}$ portfolios, we can see that the C_n^p matching strategy results in the smallest VaR (CTE) for all ages 20 to 60, which supports the claim that the C_n^p strategy has a better performance in mortality immunization.

Figure 5.11: 5% VaR and 5% CTE of the portfolio surplus at time 0

5% VaR (left column)

5% CTE (right column)

(a) ${}_{20}PFL^{TP}$

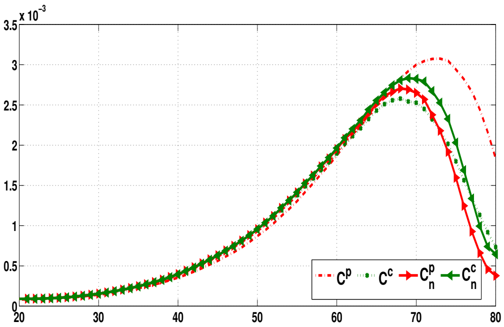

(b) ${}_{20}PFL^{TP}$

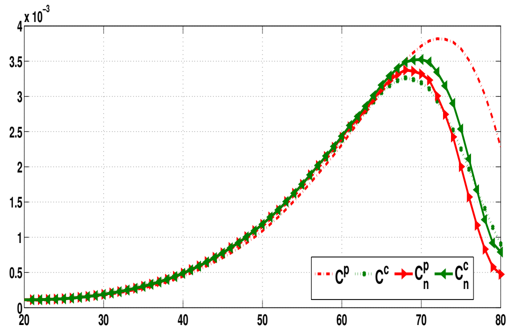

(c) ${}_{20}PFL^{WA}$

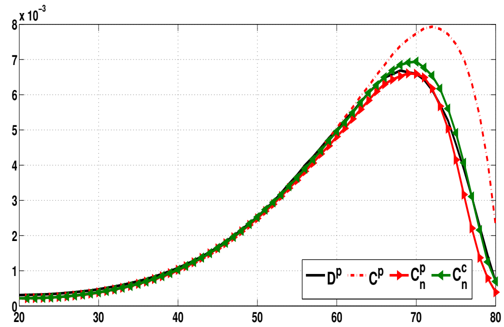

(d) ${}_{20}PFL^{WA}$

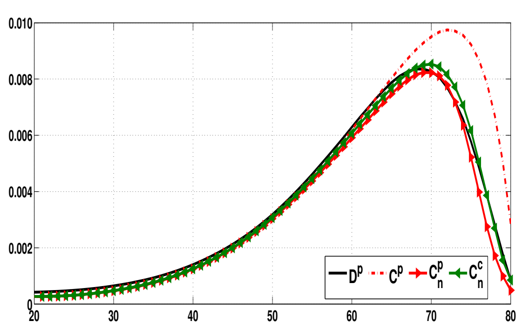

(e) ${}_{65-x}PFL^{TP}$

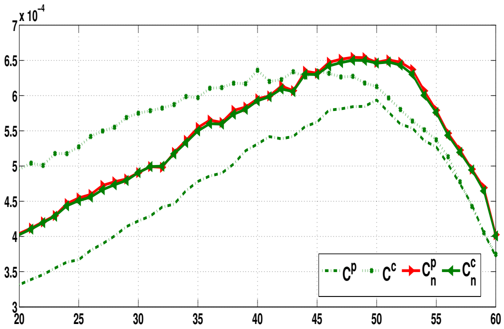

(f) ${}_{65-x}PFL^{TP}$

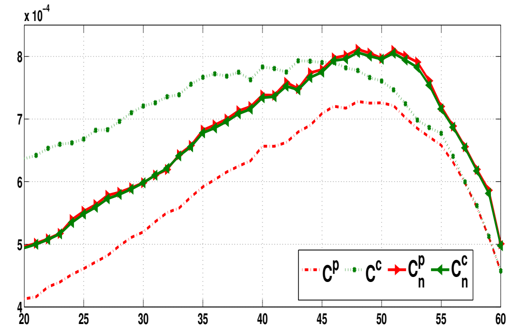

(g) ${}_{65-x}PFL^{WA}$

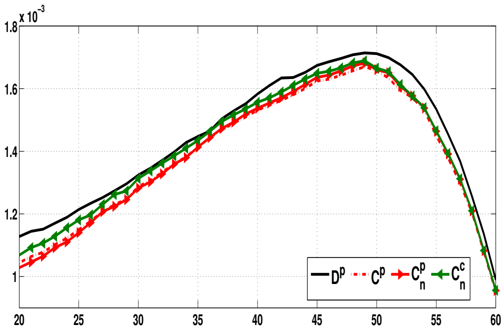

(h) ${}_{65-x}PFL^{WA}$

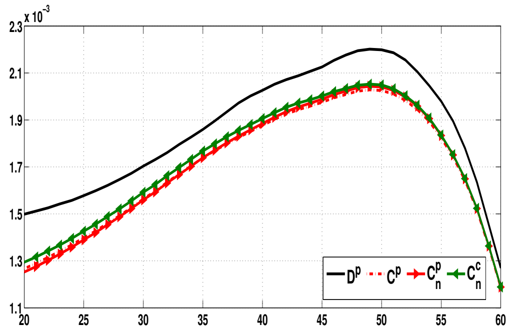

5.4 Hedging performances at time t

In this section, we compare the hedging performances of different strategies with the 5%-VaR against time t, where t is from 0 to the end of the term. For illustrations, we select age 25 to represent the young age group and age 45 to represent the mid-age group. The same four candidates are selected for each of the four portfolios for the performance comparisons as the ones in Section 5.3.2. Standing at time t, we know the realized mortality rates for the past t years; therefore, we use the retrospective method to calculate the portfolio surplus. By the retrospective method, the expected portfolio surplus at time 0 is 0. However, in order to be consistent with the results shown in Section 5.3.2, we use the prospective method to calculate the portfolio surplus at time 0 with the simulated stochastic future mortality rate sequences. We take the portfolio surplus from the C_n^p matching strategy as the base; then we obtain the ratio of the portfolio surplus from each of the other three matching strategies to the base one. For example, if the ratio of C^p to C_n^p is under (over) 100%, then the performance of the C^p (C_n^p) matching strategy is better. We summarize the results from Figure 5.12 as follows.

- From subfigures (a)-(d), we find that the ranking of the four strategies according to the 5%-VaR comparison at time 0 is different from that at time $t > 0$. At time 0, we would rank the four strategies as (1) $C^p >$ (2) $C_n^c >$ (3) $C_n^p >$ (4) C^c. For $t > 0$, we can easily identify that the weights obtained from the size free strategies produce the higher 5%-VaR than the ones obtained from the non-size free strategies for the two PFL^{TP} portfolios. Comparing (a) and (c) with (b) and (d), the ratios of C^p and C^c to the base C_n^p for age 25 are higher than those for age 45 except for the ratio of C^c to C_n^p for $t = 20$ for the portfolio ${}_{20}PFL^{TP}$, which implies that the advantage of adopting the non-size free strategy is more obvious for young ages for the surpluses along time t. Although the lines produced by C_n^p and C_n^c stick together, we can carefully observe that the 5%-VaR for the C_n^p strategy is a little lower than that for the C_n^c strategy except for that at maturity. The ranking of the four strategies after time 0 is (1) $C_n^p >$ (2) $C_n^c >$ (3) $C^p >$ (4) C^c.

- From subfigures (e)-(h), we remove the big ratio value for 5%-VaR at maturity for the D^p strategy in each subfigure for better distinctions among plots. The removed ratio values for 5%-VaR are listed as follows:

Table 6. *Ratios for 5% VaR at maturity for the D^p strategy*

	age 25	*age 45*
$_{20}PFL^{WA}$	*2.71056*	*1.80052*
$_{65-x}PFL^{WA}$	*3.42072*	*1.80052*

From these four subfigures, we can first identify that the D^p strategy produces the highest and least stable 5%-VaR of the portfolio surpluses for the two PFL^{WA} portfolios for all t. However, it is hard to rank the other three strategies because the corresponding 5% VaR values are too close for age 25. For age 45, we find that the ranking of the four strategies according to the 5%-VaR comparison at time 0 is different from that at time $t > 0$, which is consistent with our findings for the PFL^{TP} portfolios from subfigures (a)-(d). The ranking of those four strategies at time 0 is (1) $C^p >$ (2) $C_n^p >$ (3) $C_n^c >$ (4) D^p. For $t > 0$, the ranking becomes (1) $C_n^c >$ (2) $C_n^p >$ (3) $C^p >$ (4) D^p. The non-size free strategies produce smaller impacts on the portfolio surpluses for $t > 0$ than the size free strategies. Furthermore, we suggest C_n^c rather than C_n^p as the best strategy according to the comparisons of 5%-VaR for $t > 0$ for the PFL^{WA} portfolios.

Figure 5.12: 5% VaR for portfolio surplus against time t

age 25 (left column) age 45 (right column)

(a) ${}_{20}PFL^{TP}$

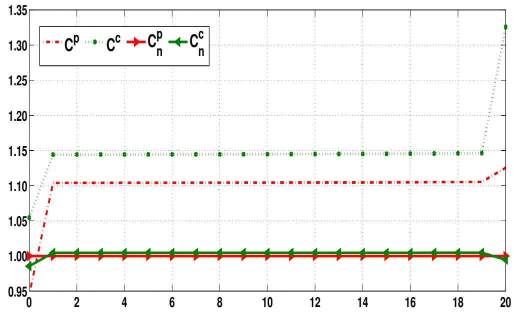

(b) ${}_{20}PFL^{TP}$

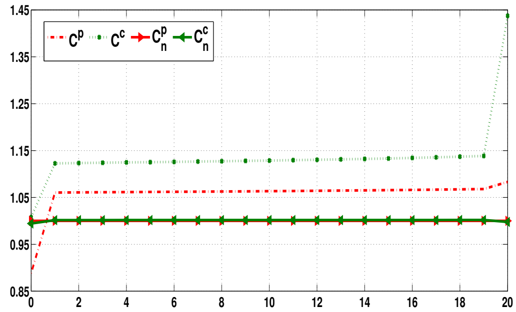

(c) ${}_{65-x}PFL^{TP}$

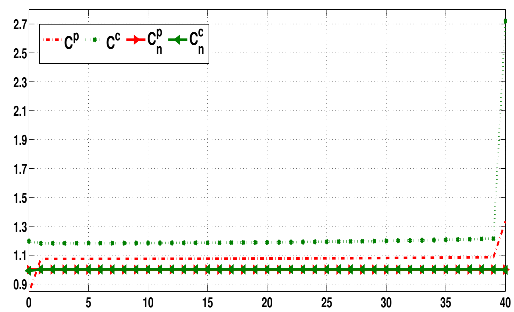

(d) ${}_{65-x}PFL^{TP}$

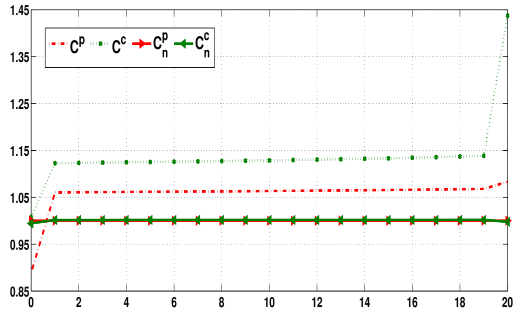

(e) ${}_{20}PFL^{WA}$

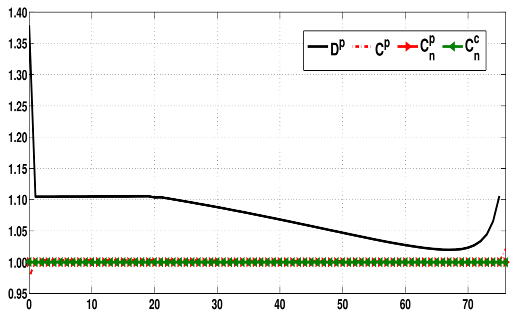

(f) ${}_{20}PFL^{WA}$

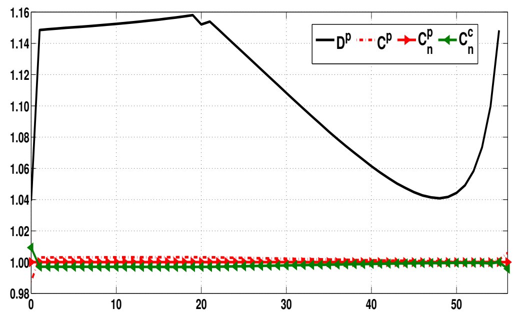

(g) ${}_{65-x}PFL^{WA}$

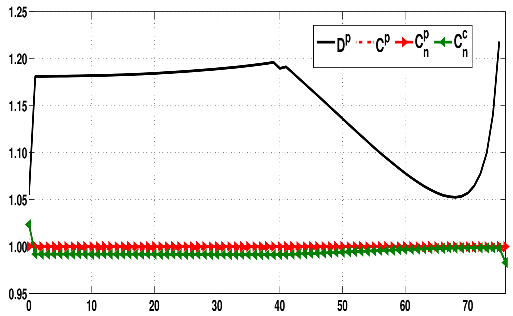

(h) ${}_{65-x}PFL^{WA}$

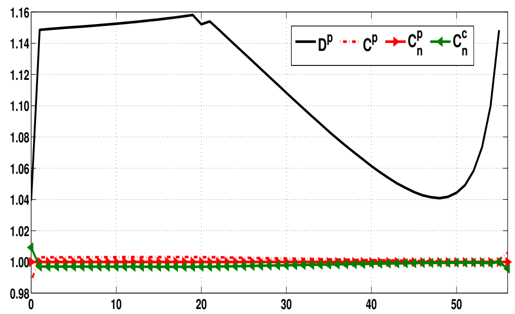

Chapter 6

Conclusion

Mortality improvement occurred over the last decades threatens the financial soundness of annuity providers, pension programs and social security systems. Other than interest rate risk, longevity and mortality risks are another essential risk factors which need to be managed effectively. As a result, there is a great importance to adopt an effective method of hedging longevity and mortality risks. Although purchasing mortality-linked securities can be used for hedging purposes, natural hedging is more preferable since there are no extra hedging costs involved. Inspired by the literature regarding to size-free matching strategies for mortality immunization and the relational models for building relationships between two mortality sequences, we develop the non-size free matching strategies for mortality immunization.

In this project, we propose nine non-size free matching strategies for each of six forms of mortality rates, μ, Q, P, $\ln(\mu)$, Q/P and $\ln(Q/P)$. These nine non-size free matching strategies can be classified into three group according to the corresponding three mortality relational models: G_L (D_n^{pc}, C_n^{pc} and DC_n^{pc} from the linear relational model), G_P (D_n^p, C_n^p and DC_n^p from the proportional relational model) and G_C (D_n^c, C_n^c and DC_n^c from the constant relational model). We also prove that some strategies produce the same weights, if $U = \mu$, specifically $\hat{w}_L(D_n^{p\,c}) = \hat{w}_L(D_n^c)$, $\hat{w}_L(C_n^{p\,c}) = \hat{w}_L(C_n^c)$ and $\hat{w}_L(DC_n^{p\,c}) = \hat{w}_L(DC_n^c)$. Since the matching strategies based on the linear relational model result in the same weights as those based on the constant relational model, and the estimate of the parameter, $\hat{\beta}_k$, for the constant relational model is more stable than the estimates of the parameters, $(\hat{\alpha}_k, \hat{\beta}_k)$, for the linear relation model, we suggest that we adopt the matching strategies based on the constant relational model instead of the linear relational model for $U = \mu$.

Our findings from the numerical results confirm that allocating life insurance and annuity products in an insurance portfolio with the proposed non-size free matching strategies can reduce the impact on the surplus of the portfolio due to mortality movements. By comparing the hedge effectiveness, 5%-VaR and 5%-CTE for the surplus of the portfolio at time 0 and other time t until portfolio maturity for non-size free and size-free matching strategies, we conclude that the non-size free matching strategies are more effective in hedging longevity and mortality risks than the size free ones. According to the results obtained from the four portfolios we study, the non-size free matching strategy based on the proportional relational model, C_n^p, contributes to the highest hedging effectiveness among all size free and non-size free matching strategies.

Comparing the non-size free and size free matching strategies, the non-size free strategies generally produce better hedging performance than the size free ones; the non-size free strategies require more computational effort than the size free ones, because the relational model parameters are varying by the length of the mortality sequences and those parameters cannot be cancelled out when calculating the weights; the non-size free group yields C_n^p as top candidate consistently in four insurance portfolios we studied, while the size free group yields different strategies as top candidates in different portfolios.

Although the non-size free matching strategies can hedge the longevity and mortality risks and reduce the variance of the surplus of an insurance portfolio, we only study two portfolios, one portfolio of term life insurance and pure endowment, and the other portfolio of whole life insurance and deferred whole life annuity. Future research can be carried out to examine the hedge performance of the matching strategies proposed in the project with more practical insurance/annuity portfolios. Moreover, we did not study the systematic model error in this project; further study can be done in analyzing the impact of model error on the hedge performance by using one mortality model to forecast deterministic mortality rate sequences (U) and another model to simulate stochastic mortality rate sequences (U^*). In addition, life insurers and annuity providers may find it difficult to allocate the life insurance and annuity products with the optimal weight because of the selling pressure and market constraint. Adopting an effective method of incorporating matching strategies and buying mortality-linked securities may assist life insurers and annuity providers to hedge the mortality and longevity risks to a greater extent.

Bibliography

[1] Blake, D., Burrows, W., 2001. Survivor bonds: Helping to hedge mortality risk. *Journal of Risk and Insurance*, 68: 339-348.

[2] Cairns, A.J.G., 2013. Robust hedging of longevity risk. *Journal of Risk and Insurance*, 80: 621-648.

[3] Cairns, A.J.G., Dowd, K., Blake, D., Coughlan, G.D., 2014. Longevity hedge effectiveness: A decomposition. *Quantitative Finance*, 14: 217-235.

[4] Coughlan, G.D., Khalaf-Allah, M., Ye, Y., Kumar, S., Cairns, A.J.G., Blake, D., Dowd, K., 2011. Longevity hedging 101: A framework for longevity basis risk analysis and hedge effectiveness. *North American Actuarial Journal*, 15: 150-176.

[5] Cox, S.H., Lin, Y., 2007. Natural hedging of life and annuity mortality risks. *North American Actuarial Journal* ,11(3): 1-15.

[6] Dowd, K., Blake, D., Cairns, A.J.G., Dawson, P., 2006. Survivor swaps. *Journal of Risk and Insurance*, 73: 1-17.

[7] Hull, J., 2012. *Risk Management and Financial Institutions*. New Jersey: John Wiley & Sons, Inc.

[8] Lee, R.D., Carter, L.R., 1992. Modeling and forecasting U.S. mortality. *Journal of the American Statistical Association*, 87: 659-671.

[9] Li, J., Haberman, S., 2015. On the effectiveness of natural hedging for insurance companies and pension plans. *Insurance: Mathematics and Economics*, 61: 286-297.

[10] Li, J.S.H., Hardy, M.R., 2011. Measuring basis risk in longevity hedges. *North American Actuarial Journal*, 15 (2): 177-200.

[11] Li, J.S.H., Luo, A., 2012. Key q-duration: A framework for hedging longevity risk. *ASTIN Bulletin*, 42: 413-452.

[12] Lin, T., Tsai, C.C.L., 2013. On the mortality/longevity risk hedging with mortality immunization. *Insurance: Mathematics and Economics*, 53: 580-596.

[13] Lin, T., Tsai, C.C.L., 2014. Applications of mortality durations and convexities in natural hedges. *North American Actuarial Journal*, 18(3): 417-442.

[14] Lin, Y., Cox, S.H., 2005. Securitization of mortality risks in life annuities. *Journal of Risk and Insurance*, 72: 227-252.

[15] Menoncin, F., 2008. The role of longevity bonds in optimal portfolios. *Insurance: Mathematics and Economics*, 42: 343-358.

[16] Plat, R., 2011. One-year value-at-risk for longevity and mortality. *Insurance: Mathematics and Economics*, 49: 462-470.

[17] Tsai, C.C.L., Jiang, L., 2011. Actuarial applications of the linear hazard transform in life contingencies. *Insurance: Mathematics and Economics*, 49: 70-80.

[18] Tsai, C.C.L., Chung, S.L., 2013. Actuarial applications of the linear hazard transform in mortality immunization. *Insurance: Mathematics and Economics*, 53: 48-63.

[19] Tsai, C.C.L., Yang, S., 2015. A linear regression approach modeling mortality rates of different forms. *North American Actuarial Journal*, 19(1): 1-13.

[20] Tsai, J.T., Tzeng, L.Y., Wang, J.L, 2011. Hedging longevity risk when interest rates are uncertain. *North American Actuarial Journal*, 15 (2): 201-211.

[21] Tsai, J.T., Wang, J.L, Tzeng, L.Y., 2010. On the optimal product mix in life insurance companies using conditional value at risk. *Insurance: Mathematics and Economics*, 46(1): 235-241.

[22] Wang, J.L., Huang, H.C., Yang, S.S., Tsai, J.T., 2010. An optimal product mix for hedging longevity risk in life insurance companies: The immunization theory approach. *Journal of Risk and Insurance*, 77: 473-497.